STARS

Electronic Theses and Dissertations, 2004-2019

2012

The Effect Of Magnetic Bearing On The Vibration And Friction Of A Wind Turbine

Mark Ryan Vorwaller
University of Central Florida

Part of the Computer-Aided Engineering and Design Commons

Find similar works at: https://stars.library.ucf.edu/etd

University of Central Florida Libraries http://library.ucf.edu

STARS Citation

THE EFFECT OF MAGNETIC BEARING ON THE VIBRATION AND FRICTION
OF A WIND TURBINE

by

MARK RYAN VORWALLER
B.S. Brigham Young University, 2011

A thesis submitted in partial fulfillment of the requirements
for the degree of Master of Science
in the Department of Mechanical, Materials, and Aerospace Engineering
in the College of Engineering and Computer Science
at the University of Central Florida
Orlando, Florida

Summer Term
2012

ABSTRACT

Demands for sustainable energy have resulted in increased interest in wind turbines. Thus, despite widespread economic difficulties, global installed wind power increased by over 20% in 2011 alone. Recently, magnetic bearing technology has been proposed to improve wind turbine performance by mitigating vibration and reducing frictional losses. While magnetic bearing has been shown to reduce friction in other applications, little data has been presented to establish its effect on vibration and friction in wind turbines. Accordingly, this study provides a functional method for experimentally evaluating the effect of a magnetic bearing on the vibration and efficiency characteristics of a wind turbine, along with associated results and conclusions.

The magnetic bearing under examination is a passive, concentric ring design. Vibration levels, dominant frequency components, and efficiency results are reported for the bearing as tested in two systems: a precision test fixture, and a small commercially available wind turbine. Data is also presented for a geometrically equivalent ball bearing, providing a benchmark for the magnetic bearing's performance. The magnetic bearing is conclusively shown to reduce frictional losses as predicted by the original hypothesis. However, while reducing vibration in the precision test fixture, the magnetic bearing demonstrates increased vibration in the small wind turbine. This is explained in terms of the stiffness and damping of the passive test bearing. Thus, magnetic bearing technology promises to improve wind turbine performance, provided that application specific stiffness and damping characteristics are considered in the bearing design.

ACKNOWLEDGMENTS

TABLE OF CONTENTS

LIST OF FIGURES

LIST OF TABLES

CHAPTER 1: INTRODUCTION

World-wide demands for sustainable energy have resulted in increased interest in wind turbine technology. Therefore, despite widespread economic difficulties, global installed wind turbine power increased by over 20% in 2011 alone [1].

Magnetic bearing technology has recently been proposed to improve wind turbine performance by mitigating vibration and reducing frictional losses. While magnetic bearing has been shown to reduce friction in other applications, little data has been presented to establish its effect on vibration and friction in wind turbines. Therefore, the following study presents a functional method for experimentally evaluating the effect of a magnetic bearing on the vibration and efficiency characteristics of a wind turbine, along with associated results and conclusions.

The magnetic bearing under examination is a passive magnetic bearing based on a design studied at NASA [2]. This bearing was manufactured at the University of Central Florida by a group of mechanical engineering senior design students during the 2011-2012 academic year. Overall vibration levels, dominant frequency components, and efficiency results are reported for this bearing, as well as for a geometrically equivalent ball bearing, providing a benchmark for the magnetic bearing's performance. Figure 1 shows the magnetic and ball bearing test subjects.

Left: Magnetic bearing suspends rotor using magnetic repulsion
Right: Ball bearing physically supports rotor

Figure 1: Magnetic and Ball Bearing Test Subjects

Experiments on these bearings were performed in two different systems: a precision test fixture, and a small commercially available wind turbine. Figure 2 and Figure 3 graphically illustrate the test fixture and small wind turbine respectively.
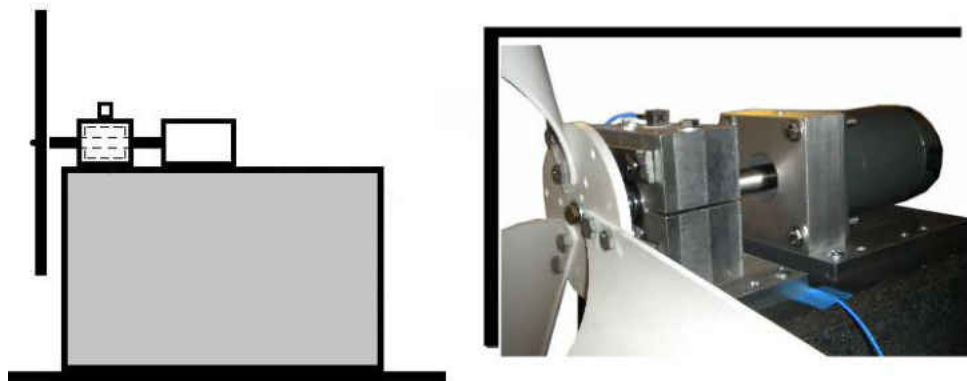
Left: Schematic of the precision test fixture
Right: Photograph of the test fixture, equipped with motor and blades

Figure 2: Visual Representations of the Precision Test Fixture
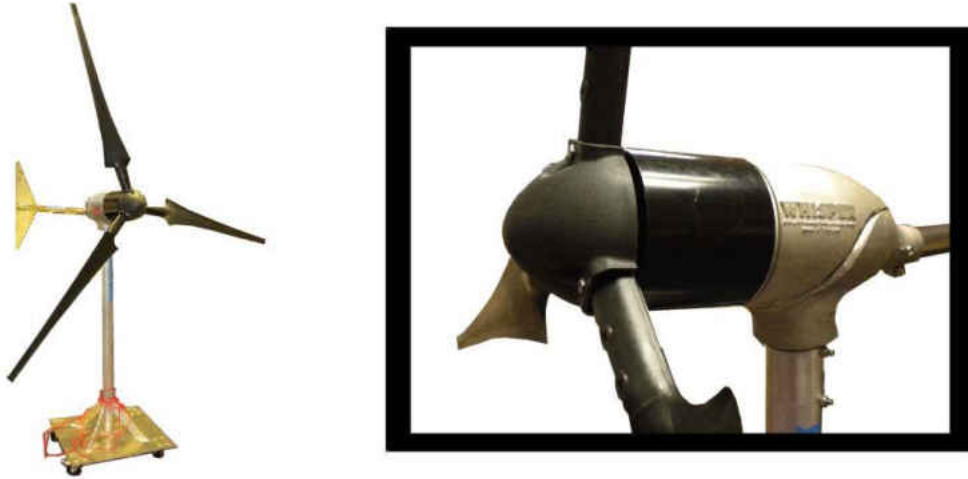
Left: Photograph of full Whisper 100 wind turbine
Right: Close-up of Whisper 100 hub and blades

Figure 3: Commercially Available "Whisper 100" Wind Turbine

Vibration and efficiency data is reported for both the magnetic and ball bearings as tested in the test fixture and small wind turbine under various wind conditions. The magnetic bearing is shown to reduce frictional losses as predicted by the original hypothesis. However, while reducing vibration in the precision test fixture, the magnetic bearing demonstrated increased vibration in the small wind turbine. This is explained in terms of the low stiffness and damping of the passive magnetic bearing. Consequently, it is concluded that application specific stiffness and damping characteristics must be considered in the bearing design if magnetic bearing is to have the desired results.

Additional discussion of this study's experimental methods, results, and conclusions is now preceded by additional background and literary review sections, facilitating a better understanding of the research for less-familiar readers.

3

CHAPTER 2: BACKGROUND

The following discussion provides background material related to topics supporting a more complete understanding of this study. These topics include rotating machinery, wind turbine technology, vibration basics, and magnetic bearing concepts.

Rotating Machinery

Rotating machinery can be generally described as any mechanical system involving rotating parts, generally moving at high speeds. Examples include motors, machine tools, and especially applicable to this study: turbines. Because of the rotating parts, friction and vibration can be hazardous to proper machine operation. Common terms associated with the components of rotating machinery include:

- Rotor – The rotating part of the machine

- Stator – The fixed part of the machine in which the rotor rotates

- Bearing – A mechanism that constrains the relative motion of moving parts

Ball Bearings are commonly used in rotating machinery to constrain the axis of rotation of a rotor. Mechanically, this is accomplished by small balls that are allowed to roll between concentric inner and outer tracks termed *races*. The general components of a ball bearing are shown in Figure 4.

Figure 4: Components of a generalized ball bearing

Wind Turbine Technology

Wind turbines are an appropriate example of rotating machinery. The previously discussed components of rotating machinery, as they apply to a common wind turbine are identified below in Figure 5.
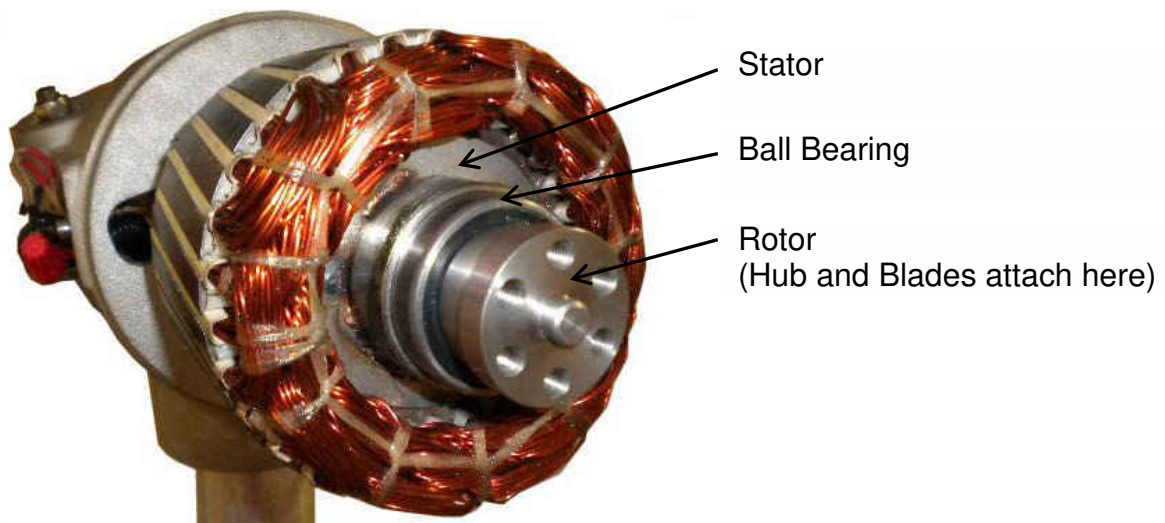
Figure 5: Components of Rotating Machinery Applied to Wind Turbine

Wind turbines are used to transform wind energy into electricity. As wind action causes the turbine blades to spin, an attached shaft provides the mechanical work required for a generator to produce electricity. Wind turbines exist in a variety of forms, most commonly classified into two main categories: horizontal and vertical axis wind turbines. *The wind turbines used in this study are horizontal axis wind turbines.* Figure 6 visually demonstrates the difference between these two wind turbine types.
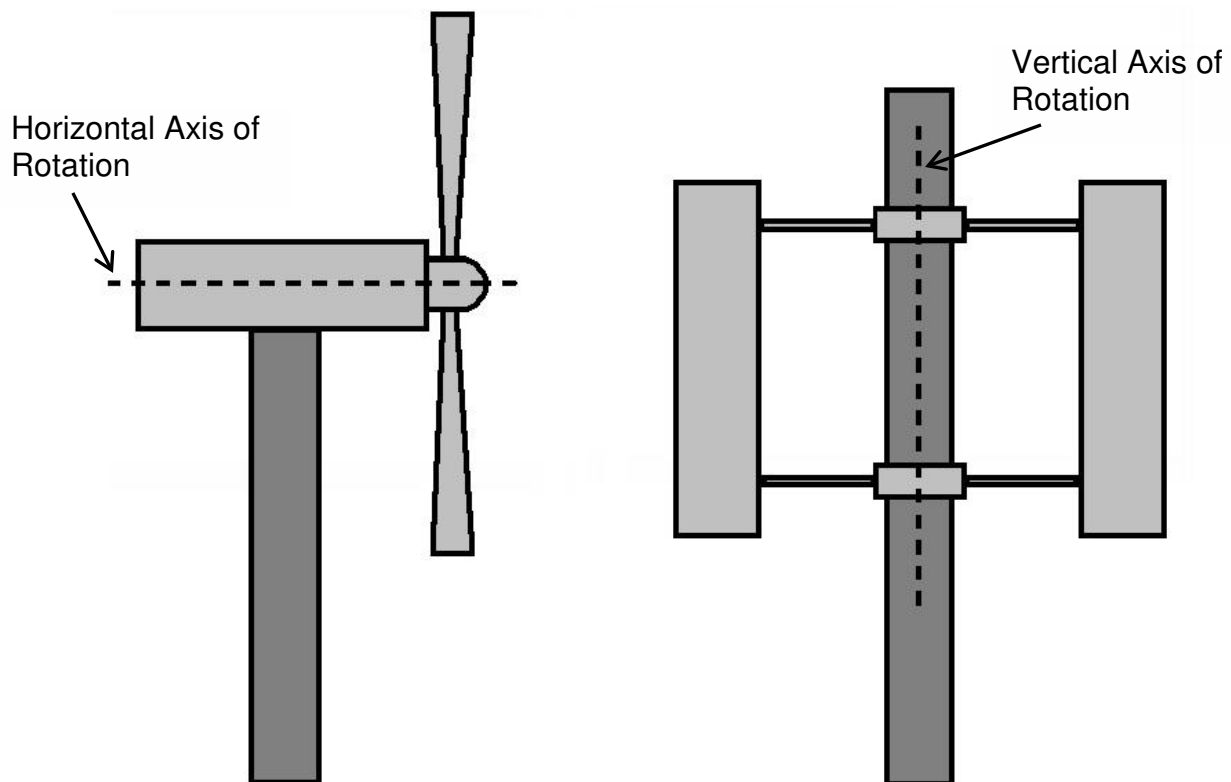
Left: Horizontal Axis Wind Turbine
Right: Vertical Axis Wind Turbine

Figure 6: Comparison of Horizontal and Vertical Axis Wind Turbines

Vibration Basics

Vibration involves mechanical oscillations about an equilibrium point, and assuming a dynamically stable system, can continue only in the presence of a forcing mechanism. In the case of rotating machinery, long-term forcing mechanisms are always present at least in the form of mass unbalances in the rotor [3]. In wind turbines, vibration is also influenced by gyroscopic effects and wind disturbances.

Wind turbine designers are concerned with vibration levels because of their effect on turbine life. Potentially damaging peak vibration amplitudes induced by wind disturbances must be considered. Thus, a means of analyzing and mitigating wind turbine vibration over a wide range of operating speeds and wind conditions is essential.

The vibration studied in this research involves the orbital motion of the rotor spin axis in the radial plane, known as lateral rotor vibration (LRV) [3]. Figure 7 identifies this plane in which lateral rotor vibration occurs.
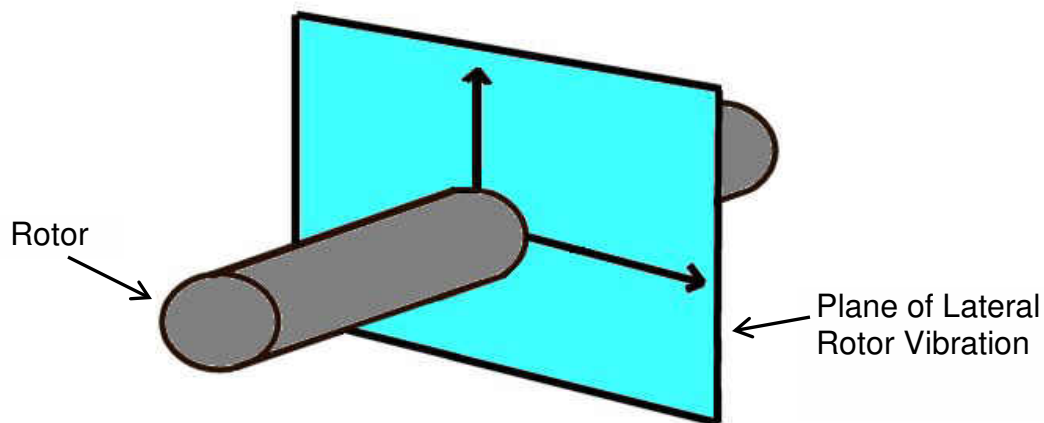
Figure 7: Plane of Lateral Rotor Vibration

The characteristics of a wind turbine's LRV are significantly affected by dynamic beam bending type deflections in the rotor. Generally, these bending type deflections are most significant when the ratio of bearing to rotor stiffness is high [3]. Therefore, proper selection of wind turbine bearings is essential to ensuring that vibration levels remain within acceptable levels.

A simple single mass system helps provide a basic understanding of the fundamental vibration concepts of stiffness and damping. Figure 8 gives an example of such a system, including a spring with stiffness *k*, and damper with viscous damping coefficient *c*.
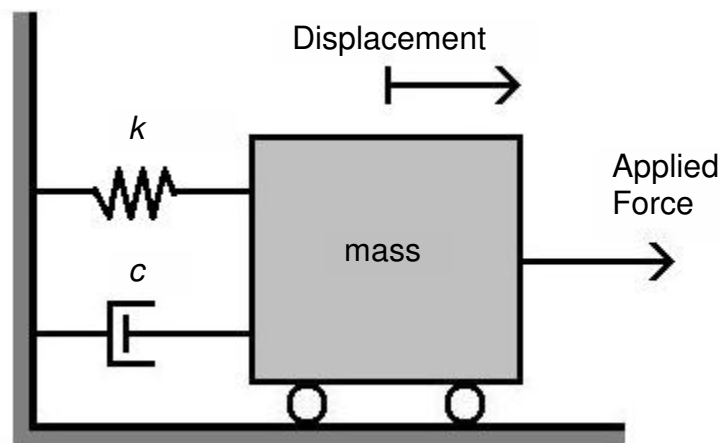
Figure 8: Simple Mass, Spring, Damper System

The system's stiffness describes the force associated with a displacement of the mass from its equilibrium point. The system's damping coefficient describes the force

associated with the velocity of the mass [4]. More complicated systems can also be described in terms of their stiffness and damping characteristics.

<h2 align="center">**<u>Magnetic Bearings</u>**</h2>

Magnetic bearings use magnetic levitation forces to stabilize a rotor without any material contact with the stator. This property not only reduces friction and wear, but eliminates the need for bearing lubricant. Additionally, bearing stiffness and damping properties can be designed to mitigate vibration effects [5]. Magnetic bearings can be broadly classified based on their design and functionality into three categories. These include active, passive, and hybrid magnetic bearings.

Active magnetic bearings use electromagnets to control the magnitude of the magnetic suspension force. This is accomplished by supplying a time-varying current to the electromagnets based on feedback from the rotor position. This allows active control of the rotor. However active magnetic bearing control systems can be costly and increase space requirements.

Passive magnetic bearings use strategically positioned permanent magnets to suspend the rotor. Common positioning approaches include the Halbach array and the use of concentric ring magnets. Figure 9 demonstrates the magnetic orientation employed by a Halbach array, the arrows pointing toward the magnets' north poles.
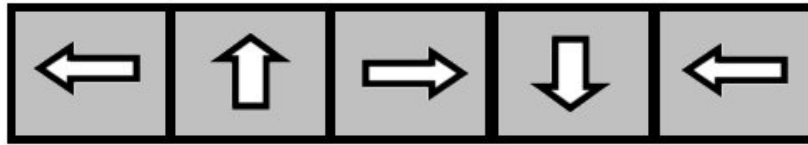
Figure 9: Halbach Array Magnet Orientation and Arrangement

Oriented as shown in Figure 9, the magnetic field cancels on the top side of the array, and strengthens on the bottom side [6]. Hence, these arrays can be concentrically wrapped around a rotor and stator such that a strong repulsive magnetic force is created between them, creating an essentially frictionless bearing. Passive magnetic bearings do not require the costly control equipment used in active magnetic bearings. However, the strength of the magnetic field is fixed and cannot be actively modified to accommodate varying operation conditions.

Hybrid magnetic bearings include bearings that employ both permanent and electromagnets in stabilizing the rotor. In general, magnetic bearings are strong candidates for improving the performance and efficiency of rotating machinery through increased power output and reduced component fatigue.

CHAPTER 3: LITERATURE REVIEW

The following review discusses significant literature and previous work related to the topic of passive magnetic bearings in wind turbines.

Passive Magnetic Bearings

Although the principles of magnetism have been applied to bearings for much longer, magnetic bearings have only relatively recently been put into practical use. Presently, dozens of companies, including Satcon Technology Corporation (Satcon), Mechanical Technology Incorporated (MTI), and Waukesha Bearings Corporation specialize in the commercial production of magnetic bearings. For example, Satcon has developed magnetic bearings for refrigeration compressors under NASA and military contracts [7]. Yet, the majority of these commercial bearings are actively controlled.

However, research on passive magnetic bearing applications has been performed. A major example is the development of passive magnetic bearing systems for flywheel energy storage. Ham, Burton, Lin, and Joo modeled the magnetic field of a Halbach array passive magnetic bearing design for a flywheel [6]. Foster-Miller Technologies studied the rotordynamics of a passive magnetic bearing system for flywheels used in space energy storage systems [8]. NASA contributed to the research effort by developing an experimental test rig for a concentric ring design passive magnetic bearing [2]. Passive magnetic bearings have also found application in artificial hearts [9].

Researchers have discussed the advantages and disadvantages of passive magnetic bearings. Generally agreed strengths of passive magnetic bearings include their near-zero friction, lower cost associated with the absence of a control system, and overall ease of maintenance. However, research has also shown that passive magnetic bearings can lack sufficient stiffness and damping to support high loads [10]. Therefore, passive magnetic bearings have been suggested for use in applications such as micro levitation systems [11].

Vibration Analysis and Rotordynamics

In general, an abundance of work has been done in the area of vibration analysis of rotors. In addition to longstanding analytical rotor models such as the Jeffcott rotor, finite element models have been proposed as a means of studying dynamic rotor properties [12, 13].

Work has also been done to better understand vibration through physical testing. Causes of rotor vibration have been shown to include misalignment, unbalance, looseness, rubbing, resonance and component wear [14]. However, the frequency spectra associated with these causes can be difficult to discern, as evidenced by Ganeriwala, Patel, Hartung's unsuccessful attempt to identify a unique frequency spectrum associated with rotor misalignment [15]. Nonetheless, vibration patterns have been shown to indicate design problems in rotating machinery [16].

Signal processing techniques have been discussed for optimal acquisition of vibration signals. Liu, Liu, Sun, and Wei presented an accelerometer based design for

measuring vibration, including a discussion of a low-pass infinite impulse response digital filter for denoising [17]. IRD Mechanalysis outlined the setup parameters that must be considered in defining a fast Fourier transform (FFT) when processing a vibration signal, including averaging type and number of averages [18].

Wind Turbine Modeling

A number of models have been developed in an effort to study the vibration of wind turbines. These models vary in complexity and purpose, ranging from simple representations of generalized masses, to intricate finite element models of wind turbine geometry.

A wind turbine rotor can most simply be described by a model of a rotating overhung disc with some degree mass unbalance. Olsson presented equations of motion for this type of system [19]. However, this model does not describe the motion of the wind turbine tower. A model of a wind turbine tower with a simplified mass nacelle and rotor was studied by Nam and Yoon [20]. Coupled models including the motion of both the wind turbine rotor and tower have been developed [21, 22].

Dozens of parameters, including blade pitch and design, can influence the vibration experienced by a wind turbine. Models have been developed to include these parameters, including a finite element model accounting for specific blade designs [23], and a full turbine model considering electrical system effects [24]. Considering the large number of parameters, data analysis methods have been studied to determine factors

having the most impact on wind turbine vibration. One such study found blade pitch to have the most significant effect [25].

CHAPTER 4: EXPERIMENTAL METHODS

Vibration and efficiency data was experimentally obtained by two general methods. First, data was recorded for the magnetic bearing housed in a specifically designed test fixture. Second, data was recorded for the magnetic bearing housed in a small commercially available wind turbine. Data from the small wind turbine offers a means of comparison for the precision test fixture. Identical experiments were also performed for a geometrically equivalent ball bearing traditionally used in wind turbines, providing a benchmark for the magnetic bearing's performance. A review of the bearing test subjects, in addition to a detailed description of the experimental methods is given.

The Test Bearings

Two geometrically equivalent test bearings were examined by this research. Specifically, this means that the surface areas between the inner and outer races of the bearings are the same. In addition, their geometry allows them to fit into the same test fixture and small wind turbine. For consistency, the bearings were coupled to the electric motor using the same coupler.

Magnetic Bearing

The main test subject is a passive magnetic bearing. Concentric neodymium rare earth ring magnets with axially magnetized poles generate a uniform repulsive

force between the inner and outer races of the bearing. Figures 10 and 11 depict the magnetic bearing geometry and corresponding magnetic field respectively.
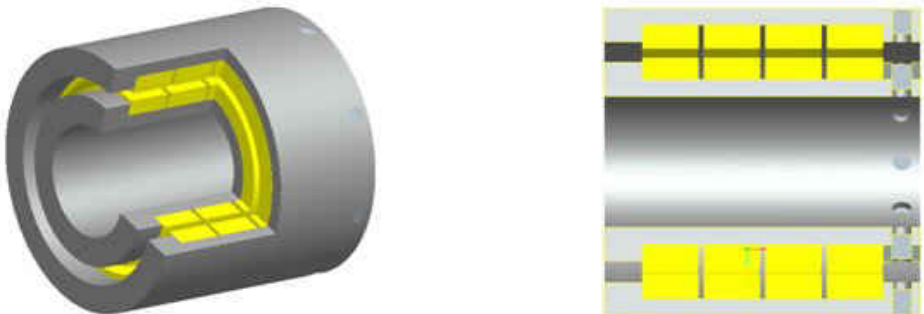
Figure 10: Geometry of the Passive Magnetic Bearing
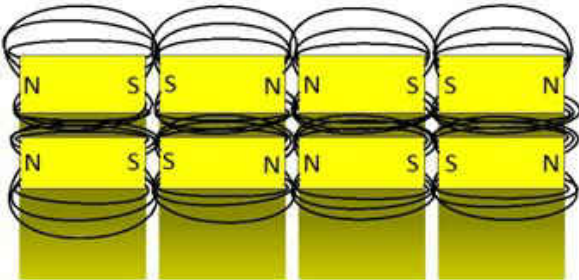
Figure 11: Magnetic Poles and Field Between Inner and Outer Ring Magnets

This magnetic portion of the bearing is positioned adjacent to a single ball bearing on one end. However, the bearing is still not axially stable, due to the tendency for the opposite poles of the ring magnets to attract when not fixed in place. Thus, the unrestrained bearing will prefer an orientation shifted by one ring magnet. Figure 12

shows the completely assembled magnetic bearing in this unrestrained shifted position,

while Figure 13 shows the bearing forced into proper alignment.

Figure 12: Completely Assembled Magnetic Bearing in Shifted Position

Figure 13: Completely Assembled Magnetic Bearing Forced into Alignment

Ball Bearing

The ball bearing test subject is composed of four adjacent deep-groove ball bearings. This bearing represents the rolling-element bearings commonly found in modern wind turbines. The bearing surface area of these four adjacent ball bearings is geometrically equivalent to the magnetic and ball bearing surface area of the passive magnetic bearing. Figure 14 depicts the ball bearing.

Figure 14: Ball Bearing Used to Benchmark Magnetic Bearing Performance

Experimental Testbed

A testbed was designed and assembled to experimentally measure the vibration and efficiency characteristics of both the magnetic and ball bearing test subjects under various wind conditions [26]. This testbed allows experiments to be performed in a more controlled environment than that common to a larger wind turbine. A schematic of the testbed is provided in Figure 15. Labeled items are identified in Table 1.
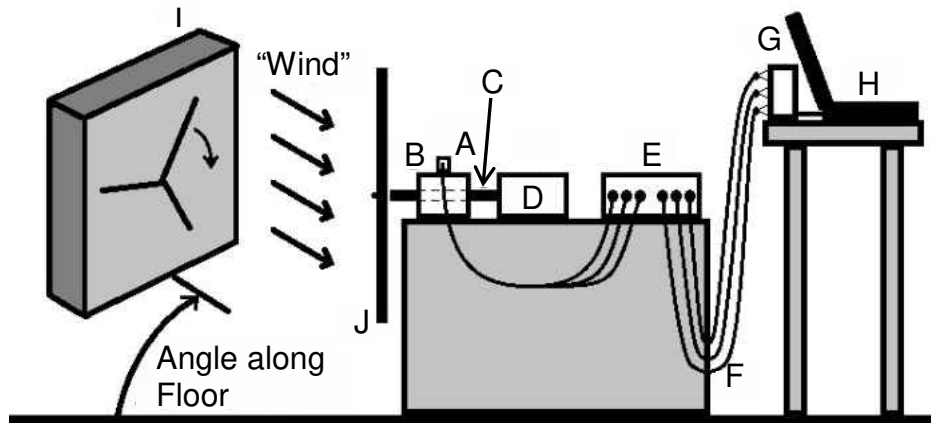
Figure 15: General Schematic of Experimental Test Set-up

Table 1: Component Details from Testbed in Figure 15

Label	Item	Details
A.	Accelerometer	ICP Accelerometer, Model #356B21
B.	Bearing Housing	6061 Aluminum, Machined at University of Central Florida
C.	Rotor	20 mm Diameter 1566 Steel Shaft
D.	Electric Motor	50 Watt DC Motor, Rated at ~0.5 Amps
E.	Signal Conditioner	PCB Electronics, Model #482C05
F.	BNC Cables	BNC to BNC
G.	USB Data Acquisition	National Instruments USB9234
H.	Computer	Dell Inspiron 8600 with XP Pro 2002, 1.5 Ghz, 1 GB, loaded with Labview 2009
I.	Fans	Industrial Fan in Custom Box
J.	Blades	16 inch Polyvinyl Chloride (PVC)

The bearing under examination is housed in an aluminum fixture, upon which is a stud-mounted 3-axis accelerometer. The bearing supports an overhung rotor, which is driven by an electric motor on its fixed end, and secured to three polyvinyl chloride (PVC) blades on its free end. The blades are mounted such that the constant angular velocity induced by the motor simulates the effect of a steady head wind. Additionally, wind disturbances from different directions can be simulated by an appropriately placed fan. The corresponding vibration is transferred to the accelerometer through the bearing fixture, providing a functional means of measuring the vibration of the rotor-bearing system. Data from the accelerometer is recorded in Labview via a signal conditioner and a USB compatible data acquisition device.

Fixture Components

The experimental testbed required the design and manufacture of a number of custom fixture and assembly components. These components are critical for proper motor, shaft, and bearing alignment, and include the bearing housing, motor mount, and bearing specific shafts. Figure 16 and Figure 17 show the CAD model and finished assembly of these particular components respectively.
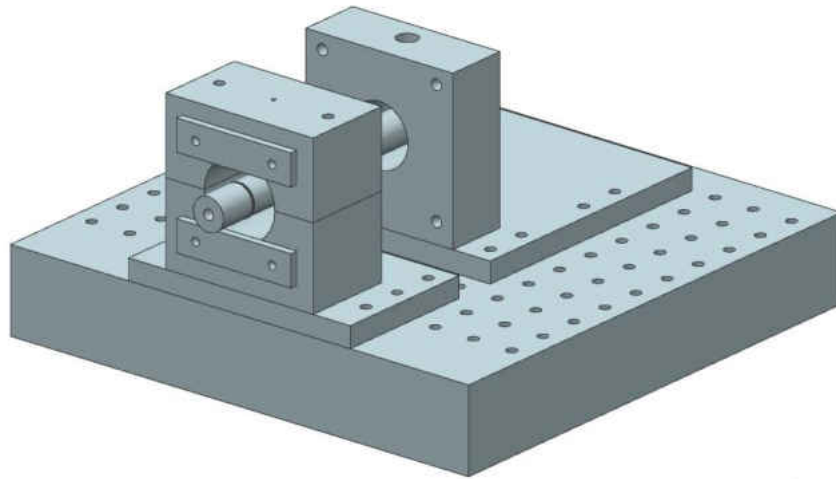
Figure 16: CAD Model of Fixture Assembly
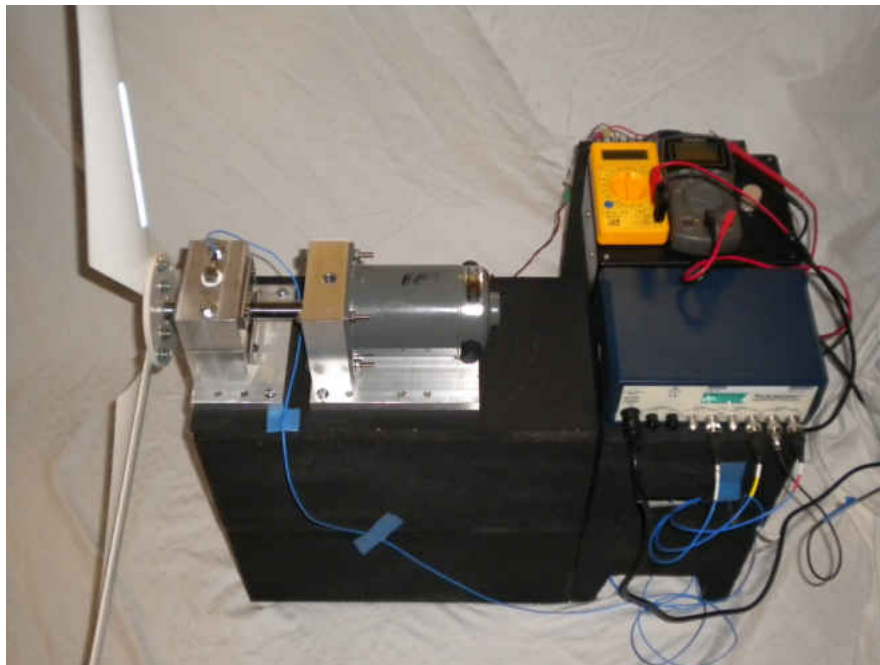
Figure 17: Photo of Finished and Wired Assembly

The components were modeled in Unigraphics NX 7.5, and manufactured at the University of Central Florida's machine shop. Component dimensions contributing to proper alignment were machined to within five thousandths of an inch tolerance. Engineering drawings for each specific part are provided in Appendix A.

Test specific shafts were machined for three general cases: magnetic bearing and geometrically equivalent ball bearing testing, reference ball bearing testing, and single bearing testing. Finished shafts in their appropriate configurations are shown in Figures 18, 19, and 20.

Figure 18: Magnetic and Ball Bearing Shaft/Coupler Configuration

Figure 19: Reference Ball Bearing Shaft Configuration

Figure 20: Single Bearing Configuration

Each shaft is designed to properly align its associated bearing in the bearing housing, decreasing the time required to switch between experiments. A set screw fixes the shaft to the motor shaft.

Wind Simulation

As mentioned previously, the electric motor causes the PVC blades to rotate at a constant rate, simulating a steady wind directed perpendicular to and towards the forward facing plane of the blades. However, the blade positioning and direction of motor rotation must be in agreement in order for this to be the case. Figure 21 shows the proper blade position and associated motor rotation for the geometry of the blades specific to this study.

Concave side of blade faces out of the page, facing an oncoming wind
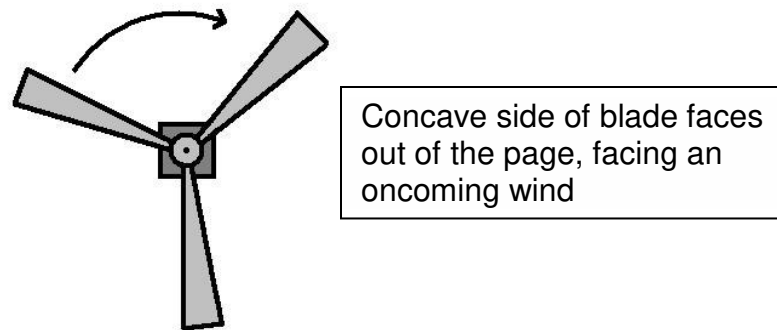
Figure 21: Blade Orientation and Rotation Direction

Tests were performed at 350, 450, and 550 RPM. These test speeds are justified by a calculation of an ideal tip speed ratio (λ) of five. The equation for tip speed ratio is defined by Equation 1, where Ω is the rotor spin speed, R is the blade radius, and v is the wind velocity [20].

$$\lambda = 5 = \Omega R / v \tag{1}$$

Assuming an approximate blade radius of one and a half feet, and an average wind of ten miles per hour, the ideal rotor rate of rotation is 468 RPM. This falls approximately in the center of the range of tested RPM.

In addition to measuring data for the system under the influence of a direct wind, steady winds and wind gusts from different angles can be simulated. This is accomplished by appropriately directing an industrial fan at the already rotating blades.

Wind gust are created by restricting the wind flow to approximately a one second

duration using a plywood/cable system. Figure 22 shows the fan.

Figure 22: Industrial Fan in Custom Housing

The angle of a wind gust is measured from a line perpendicular to the plane of

the blades. Data will be presented for wind gusts at 30 and 60 degree angles as

defined by Figure 23.
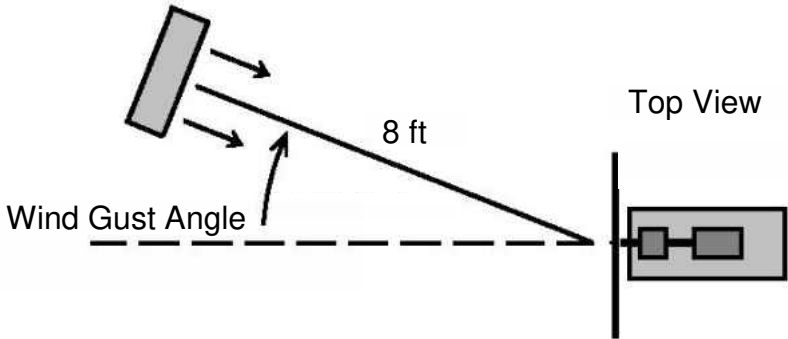
Figure 23: Wind Angle Definition

Measuring the vibration of the rotor-bearing system required the use of several commercially available electronic devices, including a 3-axis accelerometer, a signal conditioner, a USB compatible data acquisition device, and a Labview equipped computer. The following sections provide additional detail regarding these components of the measurement system.

The 3-axis accelerometer was mounted as to readily provide lateral rotor vibration data. Figure 24 defines the Cartesian directions associated with the lateral and axial components of the rotor-bearing system vibration. As lateral vibration is the primary interest of this research, axial vibration data is not presented.
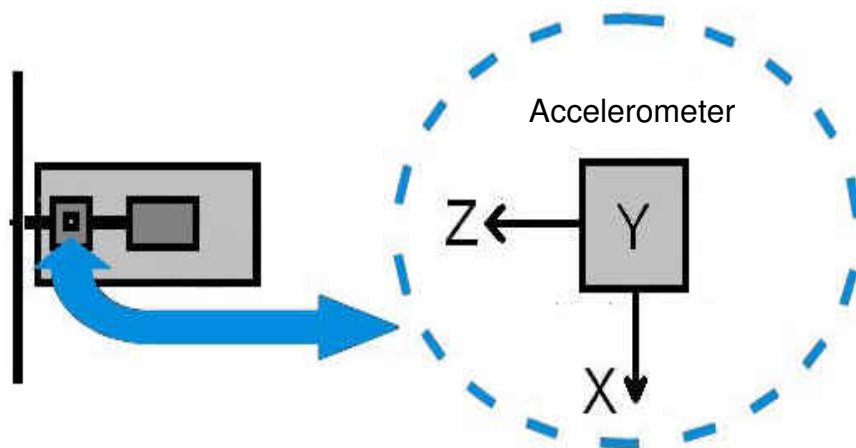
Figure 24: Accelerometer Orientation

The accelerometer requires a constant current excitation source to function properly. This constant current is provided by connecting the accelerometer to a signal

conditioner. Table 2 and Table 3 provide important specifications related to the accelerometer and associated signal conditioner. These specifications provide an understanding of the limitations of the measurement system, and thus effect the interpretation of this research's experimental results.

Table 2: Accelerometer Specifications

Specification	English Units	SI Units
Sensitivity	10.2 mV/g	1.040 mV/m/s^2
Frequency Range (Y and Z)	2 to 10,000 Hz	2 to 10,000 Hz
Frequency Range (X)	2 to 7,000 Hz	2 to 7,000 Hz

Table 3: Signal Conditioner Specifications

Specification	English Units	SI Units
Constant Current Excitation	4 mA	4 mA
Voltage Gain	1:1	1:1
Output Range	+/- 10 V	+/- 10 V

Additionally, data acquired by an accelerometer is effected by the acquisition process and subsequent signal processing. Thus, to maintain consistency, sampling parameters and signal processing techniques were maintained between experiments on the test fixture as described in Table 4:

Table 4: Sampling and Signal Processing Parameters

Parameter	Value or Description
Number of Samples	40,000
Sampling Rate	10,000 Hz
Number of Loops	5
Filter Type	Low Pass Infinite Impulse Response
Cut-off Frequency	50 Hz
Filter Topology	Butterworth, order 5
FFT Type	Magnitude - Peak
FFT Averaging	5 Linearly Weighted Averages

Efficiency Measurements

The efficiency of a bearing was defined in terms of the electrical power required to drive the corresponding rotor under given conditions. The equation for power is given in Equation 2.

$$P = IV$$ (2)

By this equation, power (P) is equal to the product of current (I) and voltage (V). Measurements were taken for these values using meters integrated into the circuitry between the motor and its power supply. This circuit is shown in Figure 25.
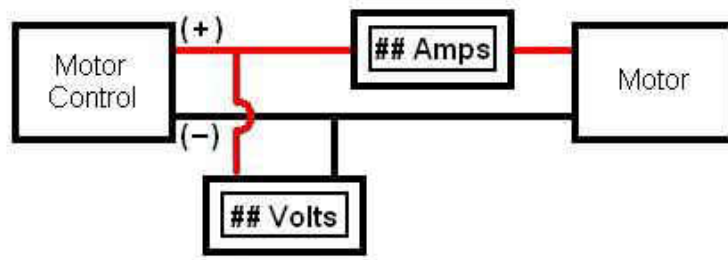
Figure 25: Circuit and Meters for Power Measurements

Whisper 100 Wind Turbine

The Whisper 100 wind turbine was used to experimentally test the magnetic and

ball bearings in a true-life wind turbine system, providing a method of analyzing and

validating the performance of the bearings in the precision test fixture.

Turbine Components

The Whisper 100 wind turbine is a self-contained small wind turbine. The

horizontal axis of rotor rotation stands five feet high and the blades have a three and a

half foot radius. The Whisper 100 was shown previously in Figure 3.

Wind Simulation

The wind simulation method used for the Whisper 100 wind turbine was slightly

different than that used for the test fixture. Because the Whisper 100 is free to rotate

about a vertical axis, it will naturally align itself with the direction of an oncoming wind.

For this reason, the influence of off-axis wind disturbances was not studied for the Whisper 100 wind turbine. An additional fan is used to account for the larger size of the turbine. Figure 26 and Figure 27 show the experimental setup associated with the Whisper 100.
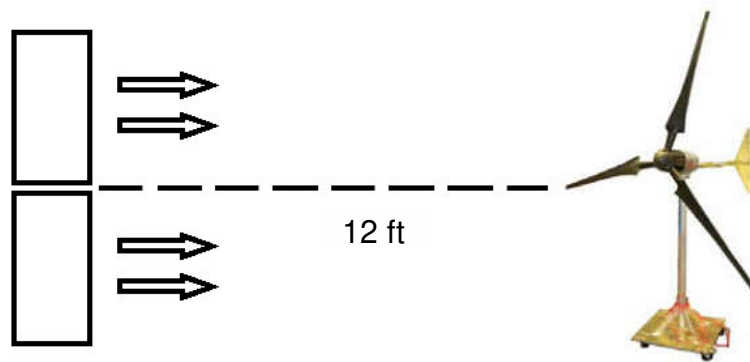
Figure 26: Schematic of Wind Simulation for the Whisper 100
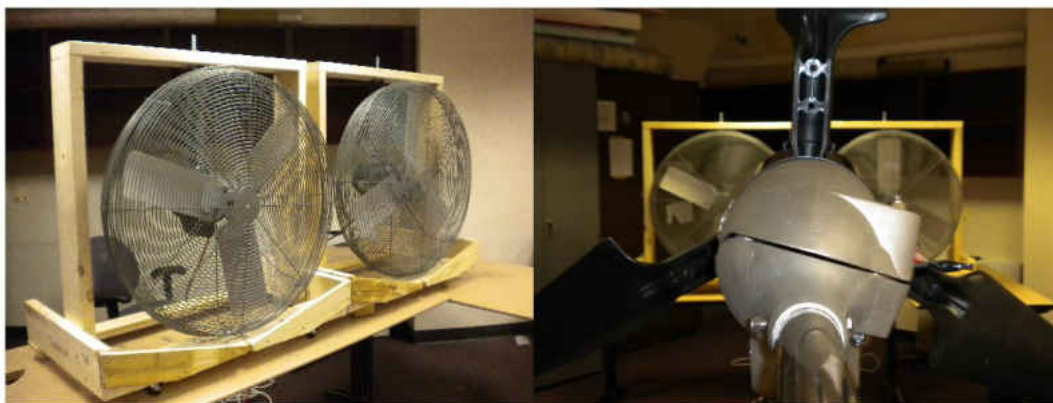
Figure 27: Photograph of Wind Simulation for the Whisper 100

Vibration Measurement Methods

The same 3-axis accelerometer was used as in the precision test fixture experiments, oriented in the same manner. However, it was mounted using a wax provided with the accelerometer. This was done as to not permanently alter the Whisper 100 wind turbine.

Efficiency Measurement Methods

Efficiency measurements were not taken in the same manner as performed on the precision test fixture. RPM values were recorded for the magnetic and ball bearings in the Whisper 100 turbine subject to the same direct wind, giving an indication of bearing friction effects.

CHAPTER 5: EXPERIMENTAL RESULTS

Overall vibration levels, dominant frequency components, and efficiency results are reported for the precision testbed and small wind turbine experiments. The effects of steady and impulse type wind disturbances are presented for the precision testbed. These results are discussed in terms of the original hypothesis that magnetic bearing will improve wind turbine performance by mitigating vibration induced by wind disturbances and reducing frictional losses.

Testbed

RMS vibration levels in the lateral directions, dominant frequency components, and efficiency results are reported for the magnetic and ball bearings as tested on the precision testbed. The effects of steady and impulse type wind disturbances are also reported.

Vibration Measurements

RMS vibration levels and dominant frequency components are reported for the magnetic and ball bearing systems. Table 5 and Table 6 present RMS vibration levels in terms of the horizontal and vertical components of lateral rotor vibration, denoted by X and Y, respectively. RPM values indicate the undisturbed speed of the motor.

Table 5: RMS Vibration Levels in X for Ball and Magnetic Bearing Systems

| RPM | Wind | X Direction RMS Vibration (g) | | % Decrease |
		Ball Bearing	Magnetic Bearing	
350	Direct Wind	0.0126	0.0112	11.4
	30° Steady	0.0159	0.0148	7.0
	60° Steady	0.0130	0.0116	10.7
450	Direct Wind	0.0139	0.0134	3.4
	30° Steady	0.0406	0.0309	24.0
	60° Steady	0.0203	0.0186	8.3
550	Direct Wind	0.0153	0.0143	6.9
	30° Steady	0.0315	0.0275	12.9
	60° Steady	0.0225	0.0200	11.0

Table 6: RMS Vibration Levels in Y for Ball and Magnetic Bearing Systems

| RPM | Wind | Y Direction RMS Vibration (g) | | % Decrease |
		Ball Bearing	Magnetic Bearing	
350	Direct Wind	0.0088	0.0075	14.6
	30° Steady	0.0101	0.0095	5.9
	60° Steady	0.0090	0.0081	9.9
450	Direct Wind	0.0096	0.0079	17.6
	30° Steady	0.0155	0.0107	30.8
	60° Steady	0.0108	0.0094	13.6
550	Direct Wind	0.0102	0.0093	9.1
	30° Steady	0.0196	0.0167	14.9
	60° Steady	0.0117	0.0102	12.7

The data in Table 5 and Table 6 supports the original hypothesis that magnetic bearing

will improve wind turbine performance by mitigating vibration. Experimentally, the

magnetic bearing reduced horizontal and vertical components of lateral rotor vibration in

each case tested. The following observations can be made from the data:

- The magnetic bearing showed average reductions of over 10 percent in X direction lateral rotor vibration.

- The magnetic bearing showed average reductions of over 14 percent in Y direction lateral rotor vibration.

- In the absence of wind disturbances, RMS vibration levels increased with rotor speed for both the magnetic and ball bearing systems.

- Vibration levels were exclusively highest under the effect of a 30 degree wind. This is due to the large component of wind contributing to the rotor velocity.

Figure 28 visually portrays the reductions in X and Y direction vibration levels in the absence of wind disturbances as established by the data in Table 4 and Table 5.
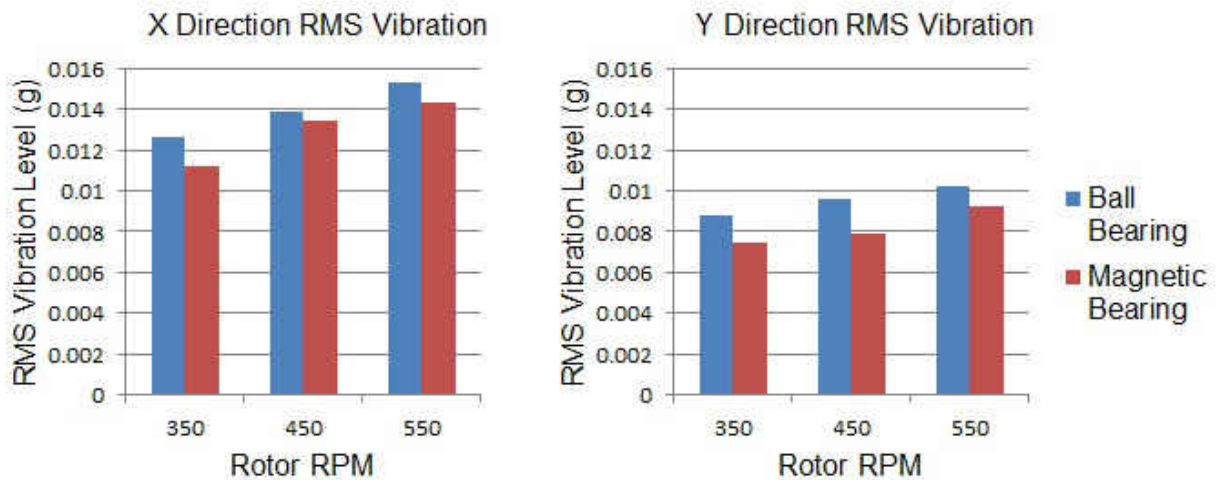
Figure 28: Magnetic and Ball Bearing Vibration Levels with No Wind Disturbance

Frequency data was also recorded for the magnetic and ball bearing systems. The resulting frequency plots confirm the trend in the RMS vibration level data, showing clear reductions in the dominant frequency components for the magnetic bearing system. Figure 29 demonstrates these reductions for the system running at 550 RPM without wind disturbances.
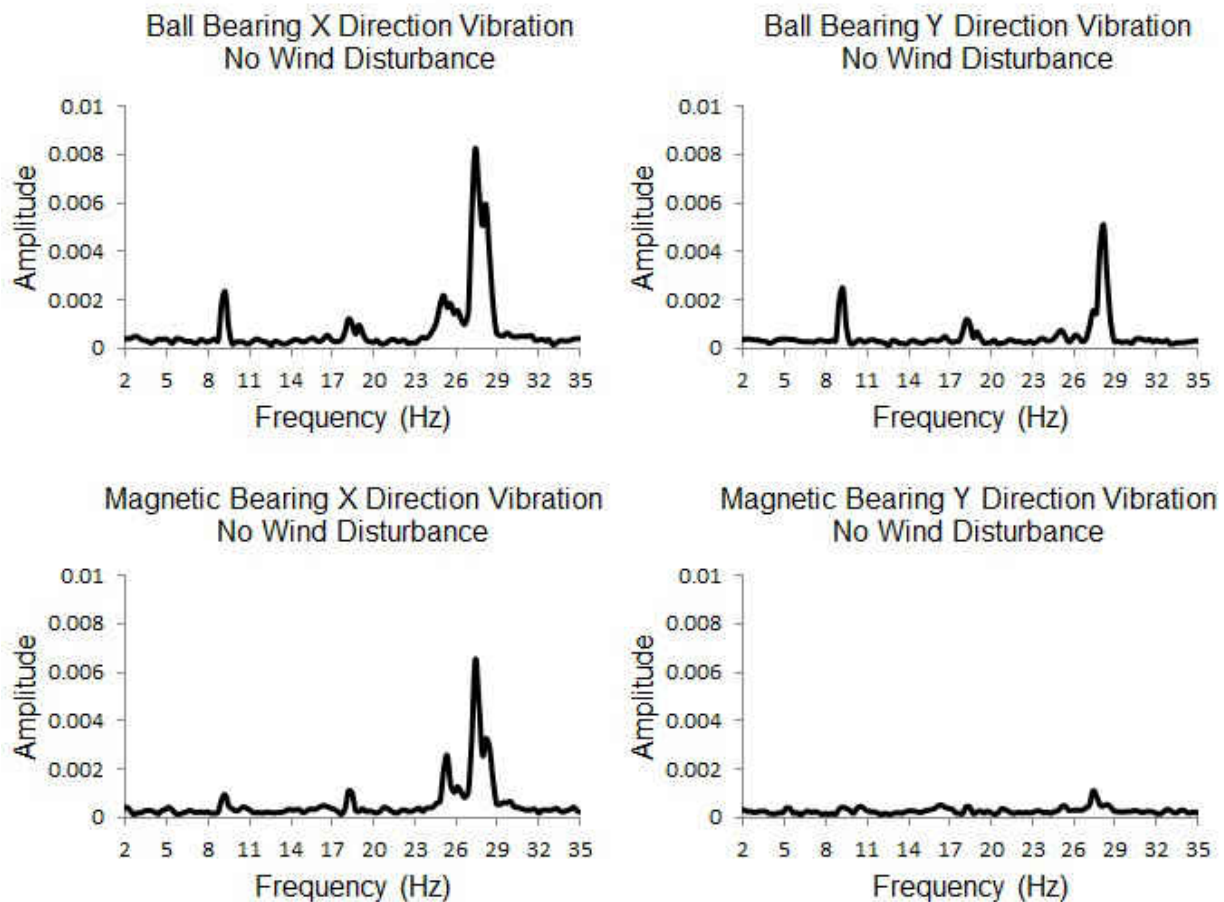
Figure 29: Frequency Plots for Magnetic and Ball Bearing Systems at 550 RPM

Figure 29 shows significant reductions in the dominant frequency components for lateral

rotor vibration at 550 RPM. The frequency plots show the largest frequency component

at three times the rotor spin speed, corresponding to the three turbine blades.

Another example of the vibration reductions attributed to the magnetic bearing is

discovered by examining the effect of a 30 degree impulse type wind gust on the lateral

rotor vibration. Figure 30 and Figure 31 show that the gust has less effect on the

vibration of the magnetic bearing than the ball bearing.
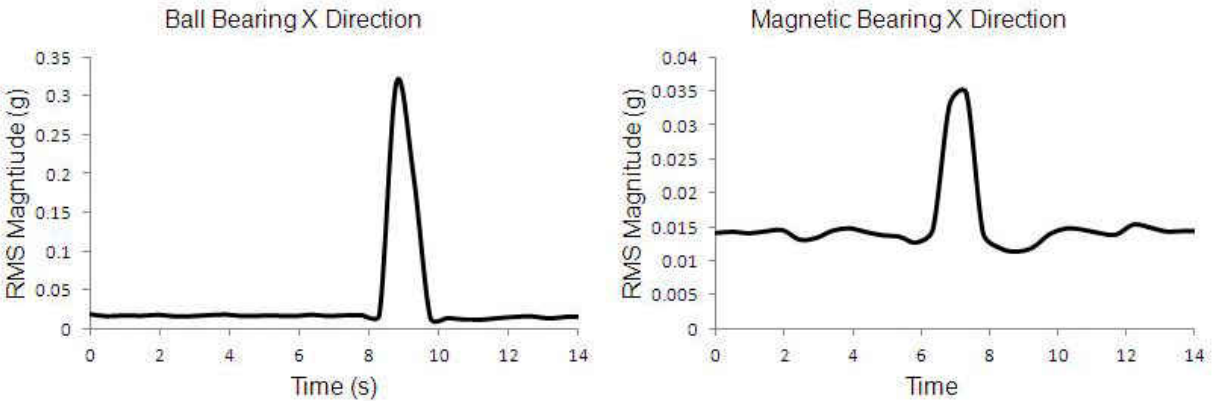
Figure 30: Impulse Response of Magnetic and Ball Bearings to a 30 degree Gust
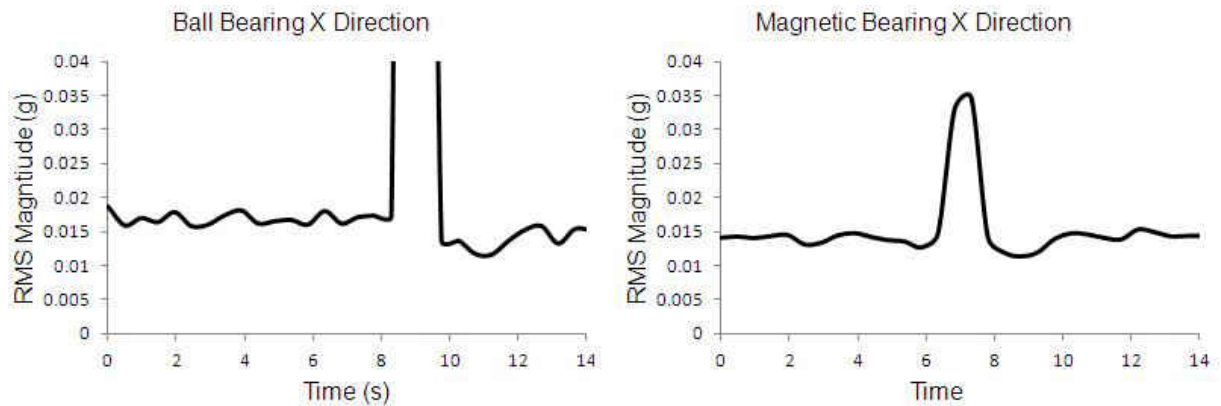
Figure 31: Zoomed View of Bearing Impulse Response to a 30 degree Gust

As expected, Figure 30 and Figure 31 show higher initial RMS values for the ball

bearing, followed by a higher response to the wind gust. This gives added support to

the suggestion that magnetic bearing will improve wind turbine performance by

mitigating vibration due to wind disturbances.

Efficiency Measurements

Table 7 reports the power required by the motor to drive the ball bearing and

magnetic bearing-rotor systems. This data was recorded at the same time as the

previously reported vibration data.

37

Table 7: Power Required by Motor for Ball and Magnetic Bearing-Rotor Systems

Wind	RPM	Power Required (Watts)		% Decrease
		Ball Bearing	Magnetic Bearing	
Direct Wind	350	21.3	15.5	27.3
	450	41.9	34.1	18.5
	550	79.5	68.0	14.5
30° Steady	350	17.2	11.7	32.4
	450	37.5	29.0	22.6
	550	72.6	59.4	18.2
60° Steady	350	20.5	15.0	26.8
	450	41.6	33.9	18.6
	550	81.0	70.3	13.2

The data in Table 7 supports the anticipated reduction in frictional losses associated with the magnetic bearing. This is demonstrated by the reduction in power required to drive the magnetic rotor-bearing system. The following specific observations can be made from the data in Table 7:

- On average, the magnetic bearing reduced the power required by the motor by over 20 percent across the investigated operational range of the turbine.

- The effect of the magnetic bearing on required power decreases with increases rotor speed.

- The magnetic bearing demonstrated the greatest power reductions for all speeds when subjected to a 30 degree steady wind. This is due to a larger component of the wind contributing to the rotation of the rotor.

Figure 32 graphically portrays the decrease in power required to drive the magnetic bearing under the tested wind conditions.
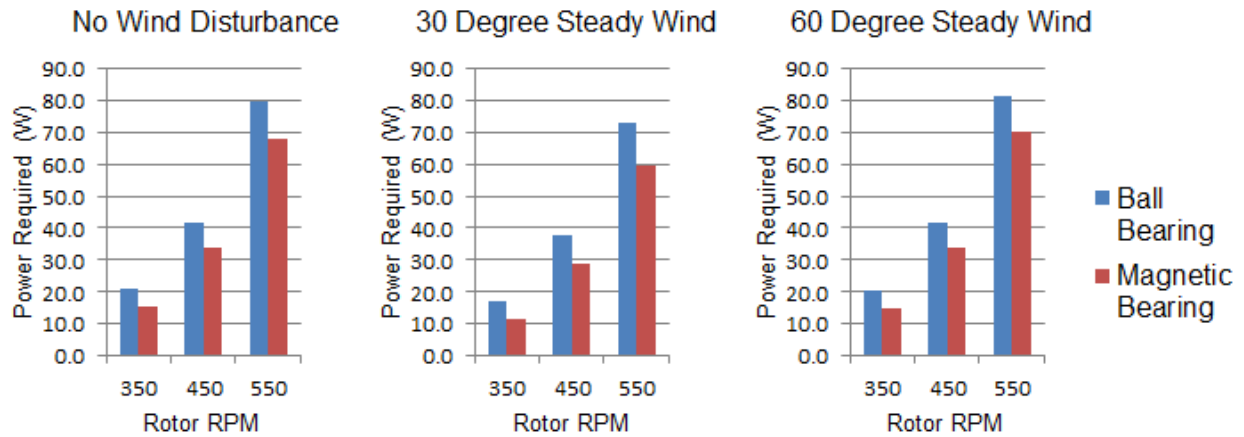
Figure 32: Comparison of Power Required by Ball and Magnetic Bearings

Whisper 100 Wind Turbine

Experimental RMS lateral rotor vibration and efficiency measurements are reported for the Whisper 100 wind turbine.

Vibration Measurements

Table 8 presents vibration levels for the magnetic and ball bearings in the Whisper 100 wind turbine under the effect of a direct wind.

Table 8: RMS Vibration Levels for Bearings in Whisper 100 Wind Turbine

		RMS Vibration (g)	
Bearing	Turbine RPM	X Direction	Y Direction
Ball Bearing	250	0.029	0.032
Magnetic Bearing	270	0.060	0.081
Percent Increase	8 %	109.4 %	154.4 %

The data in Table 8 appears to oppose the hypothesis that the magnetic bearing will mitigate vibration. This is in contrast to the results demonstrated on the precision test fixture. Additionally, the following observations can be made from the data in Table 8:

- Although the magnetic bearing allowed the wind turbine to run at a slightly higher speed, RMS vibration levels in X were over twice as large as those experienced with the ball bearing.

- RMS vibration levels for the magnetic bearing in Y were over two and a half times as large as those experienced with the ball bearing.

- RMS vibration levels were higher in Y than for X for both bearings, in contrast to the results found on the test fixture.

Figure 33 demonstrates the substantial increase in vibration experienced by the wind turbine with the magnetic bearing graphically.
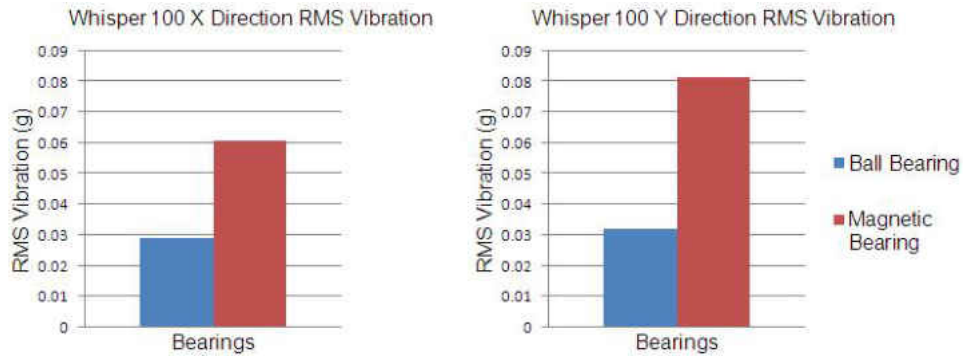
Figure 33: Vibration Levels for Bearings on Whisper 100 Wind Turbine

Figure 34 confirms that the vibration is higher in the magnetic bearing system

based on the frequency spectra of the vibration in the Whisper 100.
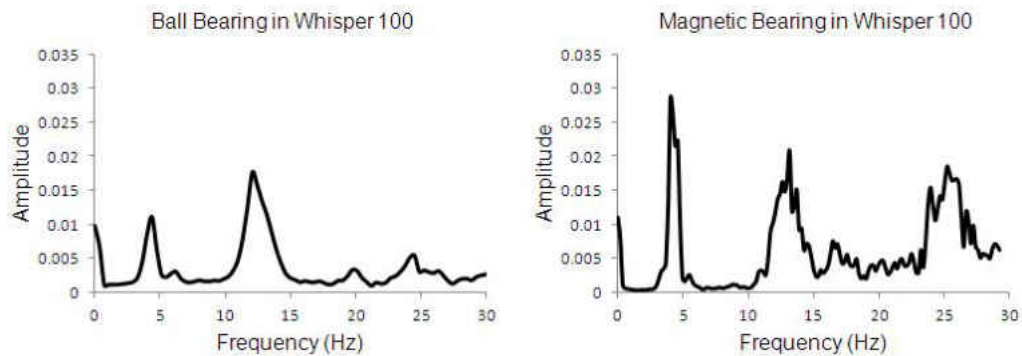
Figure 34: Frequency Spectra for Bearings in the Whisper 100 Wind Turbine

Efficiency Measurements

Power measurements were not taken on the Whisper 100 turbine, due to

substantial coverage in previous research. However, it is noted that despite the higher

41

vibration level, the Whisper 100 ran at a higher speed with the passive magnetic

bearing, confirming the expected reduction of frictional losses.

Reference Testing

Due to the contradicting results demonstrated between the vibration levels on the

test fixture and the Whisper 100 wind turbine, a reference test was run using a non-

coupled ball bearing. This test confirms that the vibration measurements on the test

fixture are due to differences in the bearings, and not alignment differences experienced

in the coupling shaft. Table 9 and Table 10 present the results of this testing.

Table 9: Reference Testing Vibration Levels in X

RPM	Wind	X Direction RMS Vibration (g)		
		Ball Bearing	Reference	Magnetic Bearing
350	No	0.0126	0.0120	0.0112
450	off-axis	0.0139	0.0135	0.0134
550	wind	0.0153	0.0152	0.0143

Table 10: Reference Testing Vibration Levels in Y

RPM	Wind	Y Direction RMS Vibration (g)		
		Ball Bearing	Reference	Magnetic Bearing
350	No	0.0088	0.0079	0.0075
450	off-axis	0.0096	0.0083	0.0079
550	wind	0.0102	0.0010	0.0093

Table 9 and Table 10 provide strong evidence that the RMS values measured on the test fixture are accurate reflections of the test bearings, and not due to misalignment in the shaft coupling. The reference bearing is on a continuous shaft, and thus would be expected to have better alignment than the coupled ball bearing. This is confirmed by the lower vibration levels in Tables 9 and 10. However, the coupled magnetic bearing still exhibits even lower vibration than both the coupled and uncoupled ball bearings, confirming the initial result that the magnetic bearing outperforms the ball bearing on the precision test fixture.

These apparently contradictory results are explained in terms of the passive magnetic bearing's stiffness and damping characteristics. Passive magnetic bearings have been shown to generally have much lower stiffness and damping than traditional ball bearings [2, 7]. Thus, in lightly loaded systems where deflections are very small, such as the precision test fixture, the lower stiffness of the magnetic bearing offers less resistance to the deflections, thereby transferring less vibration to the bearing fixture. The deflections are small enough that the bearing's low damping does not become a factor. This is supported by studies showing that relaxing bearing stiffness through critical speeds can reduce machine structure vibration [7]. On the other hand, in systems supporting higher loads where deflections may be large, such as the Whisper 100 wind turbine, the low damping provides insufficient energy dissipation. This allows the deflections, and thus vibration, to become much larger than in the ball bearing system. Therefore, magnetic bearings must be designed with wind turbine specific

43

stiffness and damping properties if they are to have the intended effect [10]. This can be accomplished by modifying the number of magnets, changing the gap distance between inner and outer races, or utilizing a hybrid or active magnetic bearing design.

Another discrepancy between the precision test fixture and the small wind turbine involved the relative magnitudes of the X and Y components of lateral rotor vibration. In the test fixture, the X component of vibration was shown to be consistently larger than the Y component. However, the opposite was shown to be true in the Whisper 100 wind turbine. This is explained in terms of the structural characteristics of the two systems. The precision test fixture does not allow motion associated with a wind turbine tower, and is subsequently more constrained in the vertical (Y) direction. Nam and Yoon showed tower and rotor vibration to be coupled [20].

CHAPTER 6: ANALYTICAL MODELING

A simple analytical model of a rotating overhung disc was used to assess the experimental results presented in this study. A graphical depiction of this four degree of freedom model is shown in Figure 35.

Where:

φ = Angle about x

θ = Angle about y
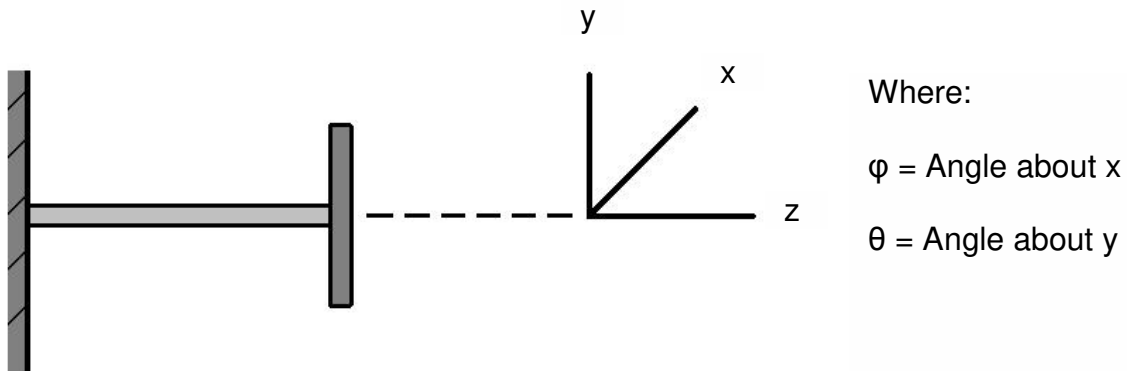
Figure 35: Model of an Overhung Rotating Rotor

The equations of motion for this model are provided in Equation 3. Parameter definitions and a derivation of Equation 3 are given by Olsson [19].

$$\begin{bmatrix} m & 0 & 0 & 0 \\ 0 & m & 0 & 0 \\ 0 & 0 & J_d & 0 \\ 0 & 0 & 0 & J_d \end{bmatrix} \cdot \begin{bmatrix} \ddot{x} \\ \ddot{y} \\ \ddot{\varphi} \\ \ddot{\theta} \end{bmatrix} + \Omega \cdot \begin{bmatrix} 0 & 0 & 0 & 0 \\ 0 & 0 & 0 & 0 \\ 0 & 0 & 0 & J_p \\ 0 & 0 & -J_p & 0 \end{bmatrix} \cdot \begin{bmatrix} \dot{x} \\ \dot{y} \\ \dot{\varphi} \\ \dot{\theta} \end{bmatrix} + \begin{bmatrix} k_3 & 0 & 0 & -k_2 \\ 0 & k_3 & k_2 & 0 \\ 0 & k_2 & k_1 & 0 \\ -k_2 & 0 & 0 & k_1 \end{bmatrix} \cdot \begin{bmatrix} x \\ y \\ \varphi \\ \theta \end{bmatrix} =$$

$$m u \Omega^2 \cdot \begin{bmatrix} \cos \omega t \\ \sin \omega t \\ 0 \\ 0 \end{bmatrix}$$

(3)

45

Equation 3 is a system of four second-order ordinary differential equations in time. However, it can be manipulated into a system of eight first-order ordinary differential equations in time by using a state space approach. First-order derivatives are defined as state variables. Then, second order derivatives can be defined as first order derivatives of these state variables. This system of eight equations is well suited for solution by Matlab's ode45 function. The Matlab code for this system and solution method is found in Appendix C. Figure 36 and Figure 37 show the analytical solutions for an overhung disc rotating at 350 and 450 RPM respectively.
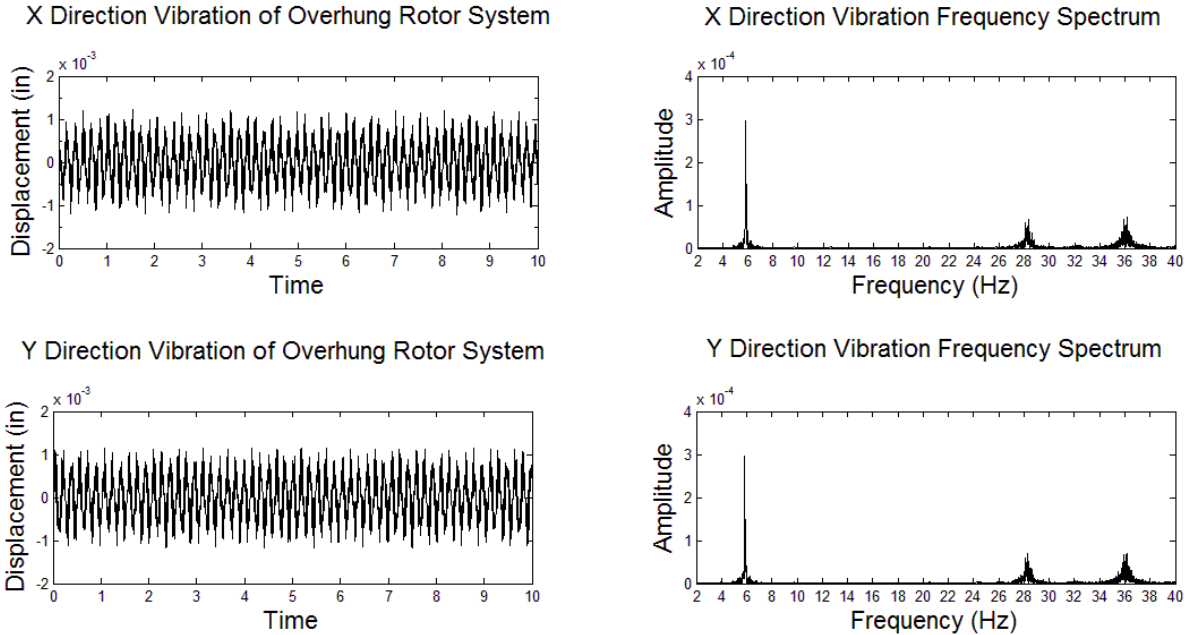
Figure 36: Analytical Solution for an Overhung Disc Rotating at 350 RPM
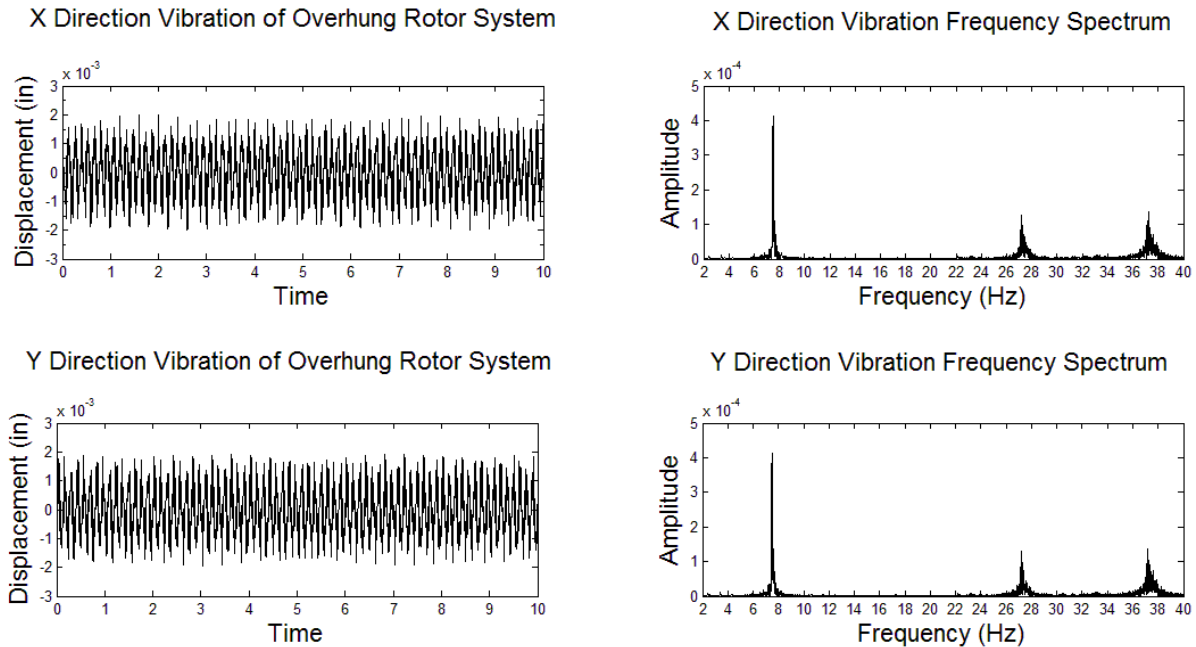
Figure 37: Analytical Solution for an Overhung Disc Rotating at 450 RPM

Although differences are noted due to simplifying assumptions, the analytical model supports the experimental results. In agreement with this study, the model shows increasing vibration levels with RPM. Additionally, the model shows a dominant frequency component corresponding to one times the rotor spin speed. A three times spin speed component would be seen if individual blade masses were included in the model. In contrast to the experimental results, the model shows symmetric X and Y direction vibration levels of the same magnitude. Harmonic frequency components in the experimental frequency spectra also differ. This is explained in terms of bearing and fixture specific characteristics not taken into account by the analytical model. However, the model provides a baseline supporting the experimental results.

CHAPTER 7: CONCLUSIONS

A functional method for experimentally evaluating the effect of magnetic bearing on wind turbine vibration and friction was successfully developed, and associated results were presented for magnetic and ball bearing test subjects in a precision test fixture and small wind turbine. Clear friction reductions, and vibration reductions dependent on application specific bearing design, support the suggested use and further study of magnetic bearing technology to improve wind turbine performance.

The data presented by this study decisively supports the expected reductions in frictional losses associated with magnetic bearing. Compared to the traditional ball bearing, the magnetic bearing was shown to significantly reduce friction in both the test fixture and the small wind turbine. These results support the proposition that passive magnetic bearings will make wind energy more economical.

Additionally, vibration results showed that magnetic bearing will mitigate wind turbine vibration, provided that application specific stiffness and damping characteristics are considered in the bearing design. For instance, while vibration due to wind disturbances was reduced by the passive magnetic bearing in the precision test fixture, vibration was shown to be higher for the magnetic bearing in the Whisper 100 wind turbine. These results were explained in terms of the passive magnetic bearing's stiffness and damping properties. Therefore, rather than discounting the possible vibration-related advantages of magnetic bearing, these results suggest the importance of carefully designing magnetic bearing properties for their specific application. Thus,

turbine-specific magnetic bearing designs are recommended to ensure the intended vibration mitigation. Suggested design variables to be considered include rotor loading, bearing air-gap distance, number, size and type of magnets. These findings also strongly advise the investigation of hybrid or active magnetic bearing designs, where bearing stiffness and damping properties can be actively controlled.

Several other fascinating directions for future work are suggested by the findings from this study. These demonstrate the value of the precision testbed to other vibration related studies. The following examples are noted:

- A study of the effects of magnetic bearing on the vibration and friction of a wind turbine using an active magnetic bearing test subject.
- Development of analytical stiffness and damping models for passive and active magnetic bearing designs.
- Establishment of vibration models considering bearing stiffness, damping, and loading relationships.
- Development of structural monitoring techniques using vibration data from the precision testbed. For example, blade deflects could be inflicted and studied.
- A study of the effect of blade design on vibration using the precision testbed.

Magnetic bearing has been conclusively shown to reduce frictional losses in wind turbine applications, and to reduce vibration provided application specific bearing designs are considered. These findings support the suggested use of magnetic bearing

technology in the effort to improve wind turbine performance, and provide motivation for

continued research in the area of magnetic bearing design for wind turbines. Such

research will allow wind power to continue to advance as an increasingly competitive

and reliable form of alternative energy.

APPENDIX A: ENGINEERING DRAWINGS
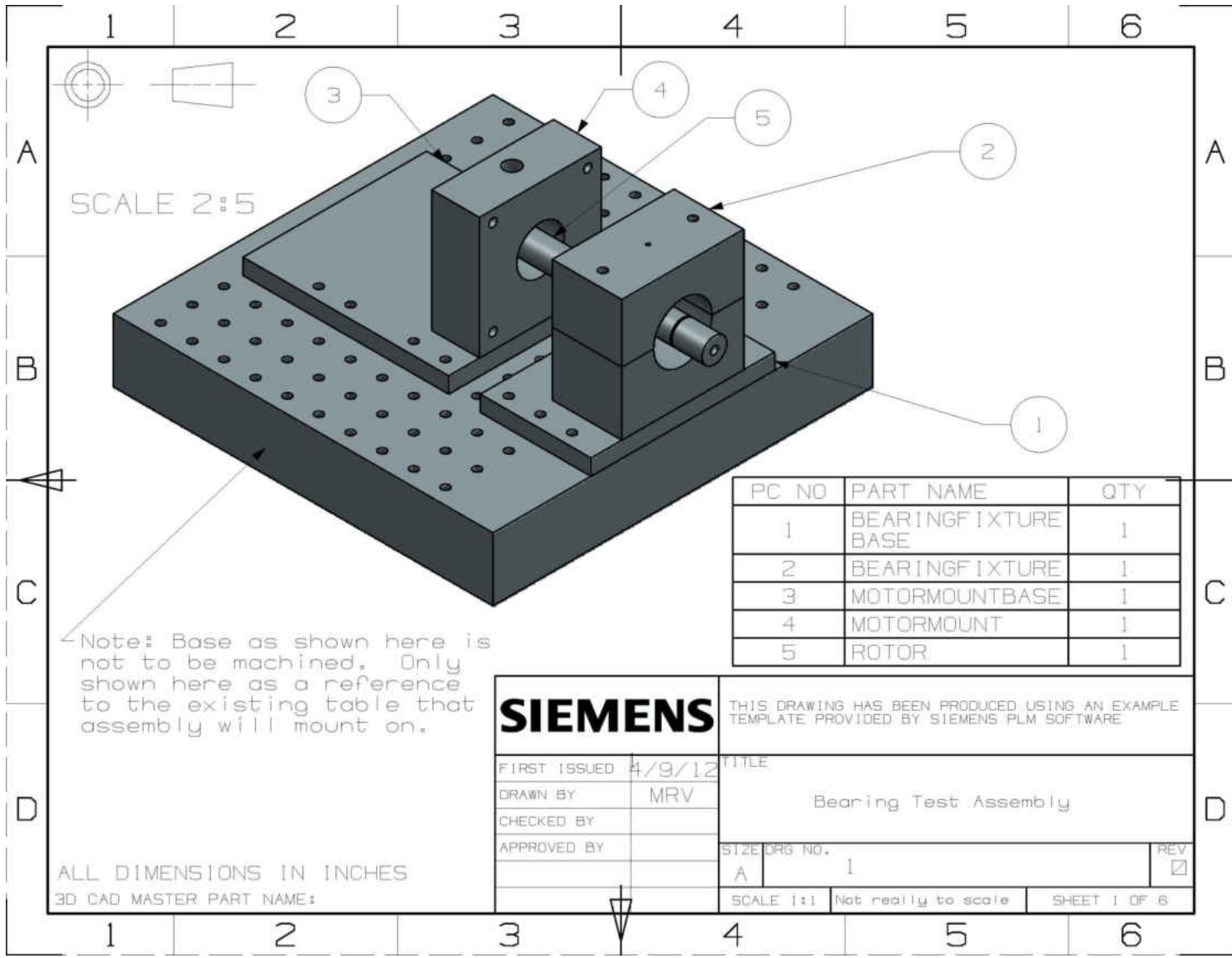
SCALE 2:5

Note: Base as shown here is
not to be machined. Only
shown here as a reference
to the existing table that
assembly will mount on.

ALL DIMENSIONS IN INCHES
3D CAD MASTER PART NAME:

PC NO	PART NAME	QTY
1	BEARINGFIXTURE BASE	1
2	BEARINGFIXTURE	1
3	MOTORMOUNTBASE	1
4	MOTORMOUNT	1
5	ROTOR	1

SIEMENS

THIS DRAWING HAS BEEN PRODUCED USING AN EXAMPLE
TEMPLATE PROVIDED BY SIEMENS PLM SOFTWARE

FIRST ISSUED	4/9/12	TITLE	
DRAWN BY	MRV	Bearing Test Assembly	
CHECKED BY			
APPROVED BY			

SIZE	DRG NO.		REV
A	1		☒

SCALE 1:1	Not really to scale	SHEET 1 OF 6

TOP

BOTTOM

0.400
1.475
4.325
5.400
5.800

3.500 +0.030
3.000
2.000
1.700
1.000
0.500

1/4" D Hole for 1/4-20 Screw.
[Bag A]. Hole not threaded.
Through entire plate.
Typical of 8 Holes.

.5" D Counter Bore.
Depth = .25 in as shown
in section view A.
Typical of 4 Holes.

0.250 +0.030
0.500

A

0.500

SECTION A-A

A

ALL DIMENSIONS IN INCHES

3D CAD MASTER PART NAME:

SIEMENS

THIS DRAWING HAS BEEN PRODUCED USING AN EXAMPLE
TEMPLATE PROVIDED BY SIEMENS PLM SOFTWARE

FIRST ISSUED 4/9/12	TITLE			
DRAWN BY	MRV	Part 1		
CHECKED BY		Bearing Fixture Base		
APPROVED BY		SIZE	DRG NO.	REV
Def. Tol. +/-.01		A	2	0
		SCALE 1:1		SHEET 2 OF 6

FRONT

TOP

BOTTOM

3.350
1.925
0.500

1.925
3.850

1.100

3.350
0.500

2.200
1.700
0.500

Hole for accelerometer.
See "Instructions for mounting
accelerometer"

Hole Threaded for 1/4-20
Screw (Bag A).
Depth = .85 in +/- 0.03
Typical of 4 Holes.

Hole for 1/4-28 Should .Bolts. Typ. of 2 Holes.

Unthreaded portion of hole for
1/4-20 Shoulder Bolts.
Typical of 2 Holes.

Cutting Plane of Seperation

Threaded with 1/4-28 Heli-Coils
to at least .75 in depth on
this bottom section of the fixture.
Typical of 2 Holes.

3.850
2.000
Ø1.850 ±0.005
2.000

0.250
1.850
2.750

SECTION C-C

This Hole will serve to fix
Bearing of same diameter
in place. The material removed
by the band saw will cause the
fit to be tight.

SIEMENS

THIS DRAWING HAS BEEN PRODUCED USING AN EXAMPLE
TEMPLATE PROVIDED BY SIEMENS PLM SOFTWARE

FIRST ISSUED	4/9/12
DRAWN BY	MRV
CHECKED BY	
APPROVED BY	
Default Tol.	+/- .01

TITLE
Part 2
Bearing Fixture

ALL DIMENSIONS IN INCHES
3D CAD MASTER PART NAME:

| SIZE | DRG NO. | REV |
| A | 3 | Ø |

SCALE 1:1   SHEET 3 OF 6

54

TOP

BOTTOM

0.400
1.975
3.825
5.400
5.800

6.500 ±0.250
4.500
3.500
1.500
1.135
0.500
0.385

1/4" D Hole for 1/4-20 Screw.
(Bag A). Hole not threaded.
Through entire plate.
Typical of 12 Holes.

.5" D Counter Bore.
Depth : .25 in as shown
in section view B.
Typical of 4 Holes.

SECTION B-B

0.250 ±0.03
0.500

ALL DIMENSIONS IN INCHES
3D CAD MASTER PART NAME:

SIEMENS

THIS DRAWING HAS BEEN PRODUCED USING AN EXAMPLE
TEMPLATE PROVIDED BY SIEMENS PLM SOFTWARE

FIRST ISSUED	4/9/12	TITLE		
DRAWN BY	MRV		Part 3	
CHECKED BY			Motor Mount Base	
APPROVED BY		SIZE	DRG NO.	REV
Def. Tol	+/- 0.01	A	4	∅
		SCALE 1:1		SHEET 4 OF 6

55

"BACK SIDE"
(SIDE INTERFACING W/ MOTOR)

0.430
1.925

3.420

"TOP"

Thru all 0.26 D hole
(Unthreaded)
Typical of 4.

"BOTTOM"

D

0.503 ±0.005
2.000 ±0.005
3.493 ±0.005
3.850 ±0.020

at least
0.150

0.610

1.500

2.755

SECTION D-D

BOTTOM

1.000
2.850
3.850

1.510
1.135
0.385

Hole Threaded for 1/4-20
Screw (Bag A).
Depth = .85 in +/- 0.03
Typical of 4 Holes.

Most important dimensions for rotor alignment are that
Hole Center is:
2 in from Bottom
1.925 in from either side
*the motor has a 2.75 D extrusion that should slide snuggly into
the outer 2.775 D indention of the mount. This should align the
rotor properly. I had trouble reverse engineering the exact
positions of outer 4 mounting holes (They were all slightly
different). But hopefully the clearance of a .26 D hole for a
1/4-20 Shoulder Bolt will be enough that things work out as
dimensioned.

"Backside" is on this (the
side of this note) side. See
Assembly Drawing to Clarify.
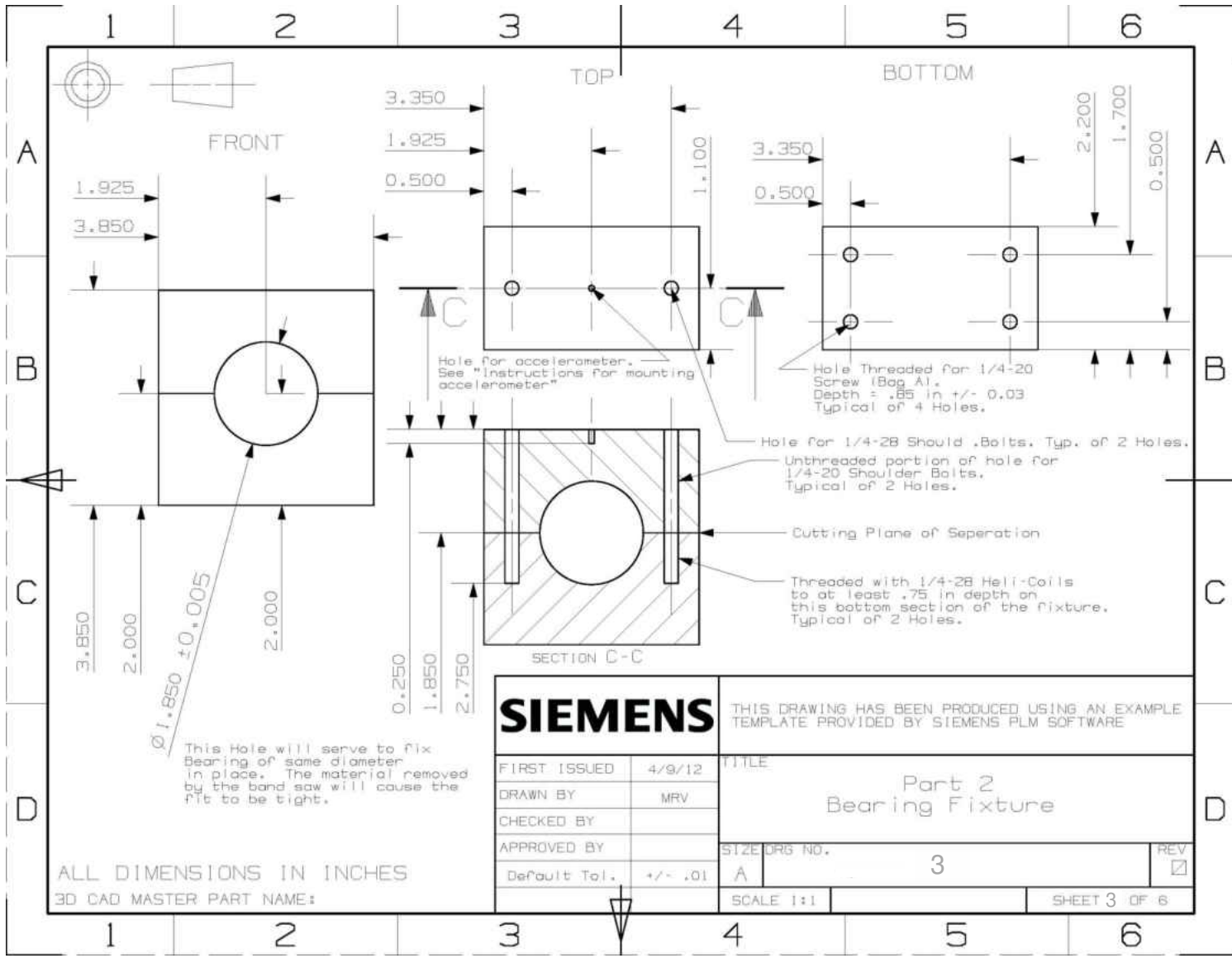
TOP

0.900
1.510

Ø0.500 ±0.050

3.850

1.925

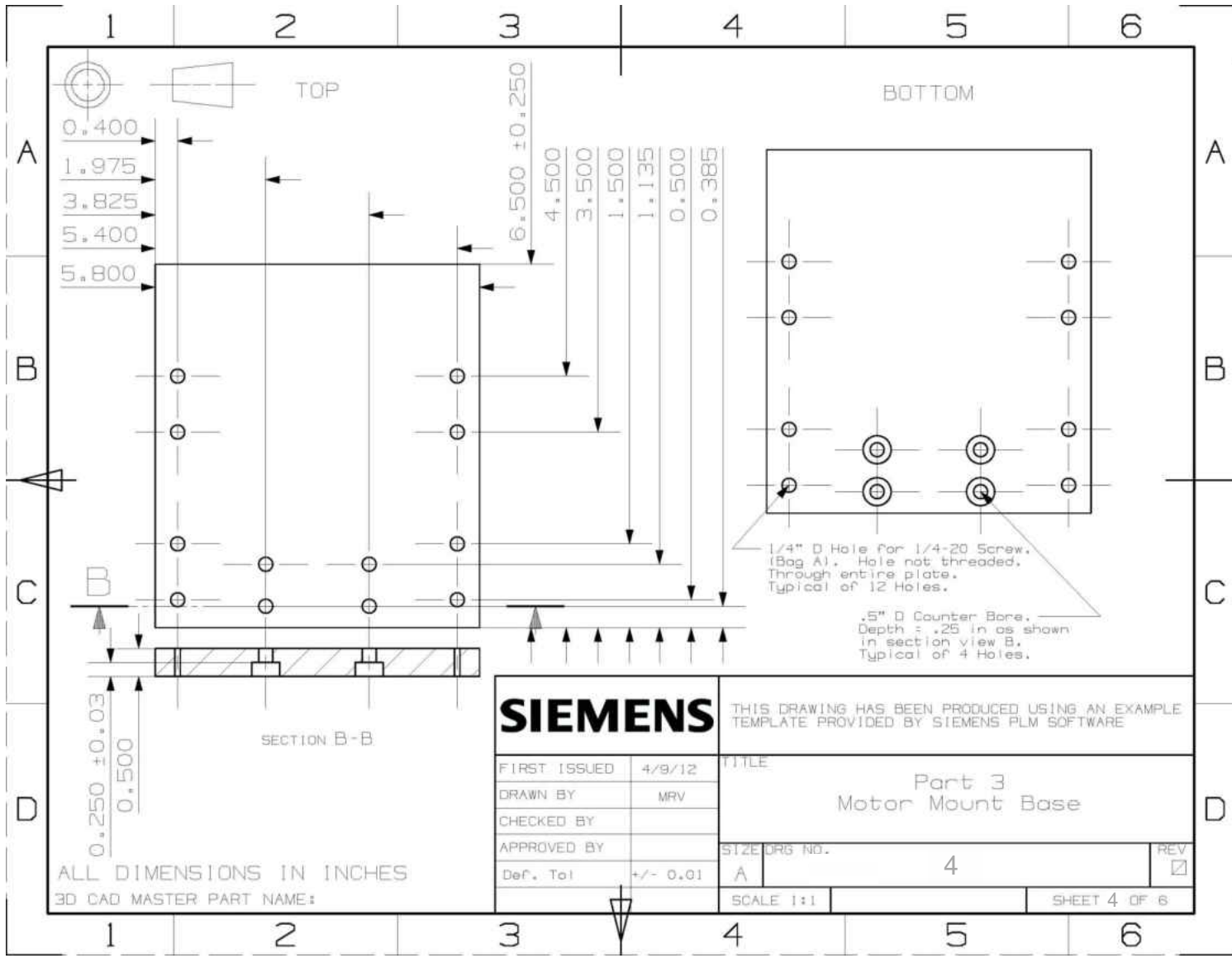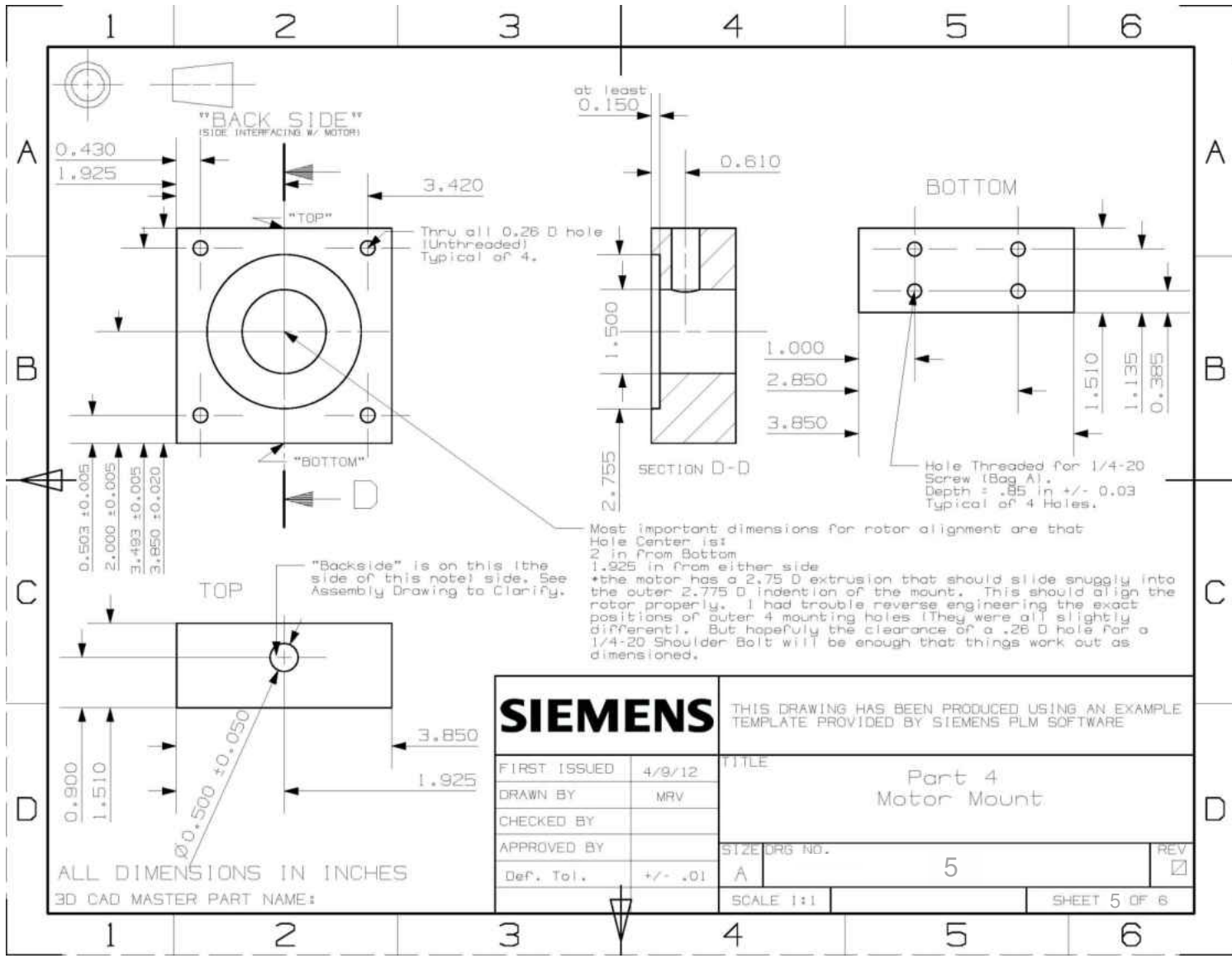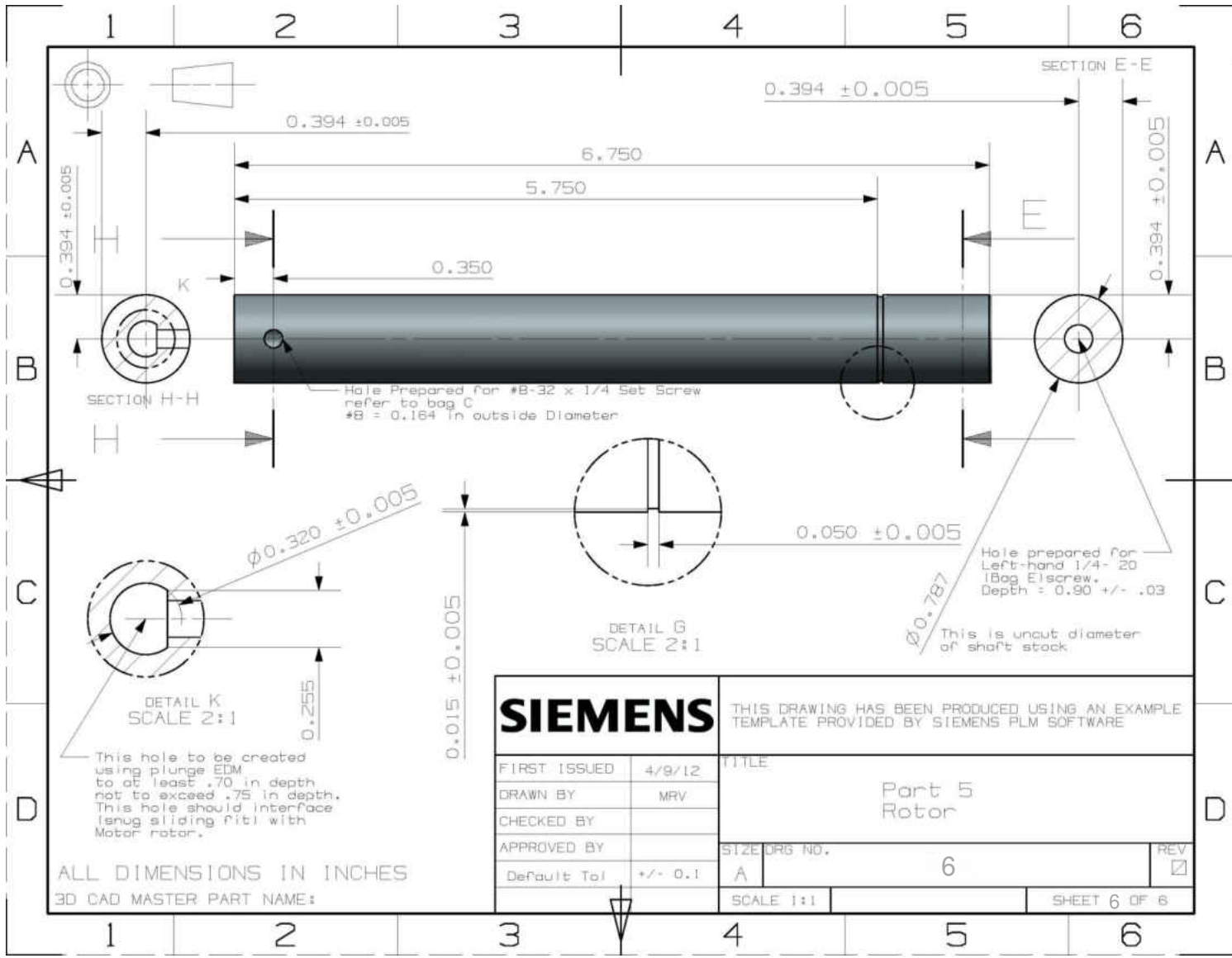ALL DIMENSIONS IN INCHES

3D CAD MASTER PART NAME:

SIEMENS

THIS DRAWING HAS BEEN PRODUCED USING AN EXAMPLE
TEMPLATE PROVIDED BY SIEMENS PLM SOFTWARE

FIRST ISSUED	4/9/12	TITLE		
DRAWN BY	MRV	Part 4 Motor Mount		
CHECKED BY				
APPROVED BY		SIZE	DRG NO.	REV
Def. Tol.	+/- .01	A	5	Ø
		SCALE 1:1		SHEET 5 OF 6

56

SECTION E-E

0.394 ±0.005

0.394 ±0.005

0.394 ±0.005

0.394 ±0.005

6.750

5.750

0.350

E

SECTION H-H

K

H

Hole Prepared for #8-32 x 1/4 Set Screw
refer to bag C
#8 = 0.164 in outside Diameter

H

DETAIL K
SCALE 2:1

∅0.320 ±0.005

0.255

0.015 ±0.005

DETAIL G
SCALE 2:1

0.050 ±0.005

∅0.787

Hole prepared for
Left-hand 1/4- 20
[Bag E]screw.
Depth = 0.90 +/- .03

This is uncut diameter
of shaft stock

This hole to be created
using plunge EDM
to at least .70 in depth
not to exceed .75 in depth.
This hole should interface
(snug sliding fit) with
Motor rotor.

ALL DIMENSIONS IN INCHES

3D CAD MASTER PART NAME:

SIEMENS

THIS DRAWING HAS BEEN PRODUCED USING AN EXAMPLE
TEMPLATE PROVIDED BY SIEMENS PLM SOFTWARE

		TITLE		
FIRST ISSUED	4/9/12	Part 5		
DRAWN BY	MRV	Rotor		
CHECKED BY				
APPROVED BY		SIZE	DRG NO.	REV
Default Tol	+/- 0.1	A	6	∅
		SCALE 1:1		SHEET 6 OF 6

57

APPENDIX B: MATLAB CODE

```matlab
%Function defining the equations of motion for the rotor system
function arrayofderivatives = SystemRotor2(t,y)

m = 0.875;
Jp = 46.055;
Jd = 23.027;
k1 = 5375000;
k2 = 1238000;
k3 = 379900;
spin = 36.65;
u = 0.05;

%Load Data from txt file created by C++ Program
% load rotorData.txt;
% A = [1:8];
% A = rotorData(:,1);
% A = single(A);

%Create variables from loaded Data
% m = A(1);
% Jp = A(2);
% Jd = A(3);
% k1 = A(4);
% k2 = A(5);
% k3 = A(6);
% spin = A(7);
% u = A(8);

%State-space representation of equations of motion
arrayofderivatives(1) = y(2);
arrayofderivatives(2) = (m*u*spin^2*cos(spin*t)+k2*y(7)-k3*y(1))/m;
arrayofderivatives(3) = y(4);
arrayofderivatives(4) = (m*u*spin^2*sin(spin*t)-k3*y(3)-k2*y(5))/m;
arrayofderivatives(5) = y(6);
arrayofderivatives(6) = (spin*-Jp*y(8)-k2*y(3)-k1*y(5))/Jd;
arrayofderivatives(7) = y(8);
arrayofderivatives(8) = (spin*Jp*y(6)+k2*y(1)-k1*y(7))/Jd;

%Ensure arrayofderivatives is a column vector for use by ode45
arrayofderivatives = arrayofderivatives(:) ;
```

```
%Set up and call ode45
y0 = [0 ; 0 ; 0 ; 0 ; 0 ; 0 ; 0 ; 0];
endtime = 100;
tspan = [0, endtime];
[t,y] = ode45('SystemRotor2', tspan, y0);

% Plot of the solution
whitebg('white')
subplot(4,1,1), plot(t,y(:,1),'black')
xlabel('Time')
h = get(gca,'xlabel');
set(h,'FontName','Arial','FontSize',12)
ylabel('Displacement (in)')
i = get(gca,'ylabel');
set(i,'FontName','Arial','FontSize',12)
title('X Direction Vibration of Overhung Rotor System')
j = get(gca,'title');
set(j,'FontName','Arial','FontSize',12)

% Plot of the solution
subplot(4,1,2), plot(t,y(:,3),'black')
xlabel('Time')
k = get(gca,'xlabel');
set(k,'FontName','Arial','FontSize',12)
ylabel('Displacement (in)')
l = get(gca,'ylabel');
set(l,'FontName','Arial','FontSize',12)
title('Y Direction Vibration of Overhung Rotor System')
m = get(gca,'title');
set(m,'FontName','Arial','FontSize',12)

% Next power of 2 from length of y1
y1 = y(:,1); %Change to do FFT on another solution {EX: y(:,3) is y disp}
L = length(y(:,1)); %Change to do FFT on another solution
Fs = L/endtime;
NFFT = 2^nextpow2(L);
Y = fft(y1,NFFT)/L;
f = Fs/2*linspace(0,1,NFFT/2+1);

% Next power of 2 from length of y3
y3 = y(:,3); %Change to do FFT on another solution {EX: y(:,3) is y disp}
L3 = length(y(:,3)); %Change to do FFT on another solution
```

```matlab
Fs3 = L3/endtime;
NFFT3 = 2^nextpow2(L3);
Y3 = fft(y3,NFFT3)/L;
f3 = Fs3/2*linspace(0,1,NFFT3/2+1);

% Plot single-sided amplitude spectrum for X
subplot(4,1,3), plot(f,2*abs(Y(1:NFFT/2+1)),'black')
title('X Direction Vibration Frequency Spectrum')
n = get(gca,'title');
set(n,'FontName','Arial','FontSize',12)
xlabel('Frequency (Hz)')
o = get(gca,'xlabel');
set(o,'FontName','Arial','FontSize',12)
ylabel('Amplitude')
p = get(gca,'ylabel');
set(p,'FontName','Arial','FontSize',12)

% Plot single-sided amplitude spectrum for Y
subplot(4,1,4), plot(f3,2*abs(Y3(1:NFFT3/2+1)),'black')
title('Y Direction Vibration Frequency Spectrum')
q = get(gca,'title');
set(q,'FontName','Arial','FontSize',12)
xlabel('Frequency (Hz)')
r = get(gca,'xlabel');
set(r,'FontName','Arial','FontSize',12)
ylabel('Amplitude')
s = get(gca,'ylabel');
set(s,'FontName','Arial','FontSize',12)
set(gcf,'Color','white')

%Compute RMS Values
columnVectorX = y(:,1);
columnVectorY = y(:,3);
rowVectorX = columnVectorX';
rowVectorY = columnVectorY';
sizeX = size(columnVectorX)
sizeY = size(columnVectorY)
numValues = sizeX(1)
squareX = rowVectorX*columnVectorX
squareY = rowVectorY*columnVectorY
rmsX = sqrt(squareX/numValues)
rmsY = sqrt(squareY/numValues)
```

LIST OF REFERENCES

[1] Sawyer, S., & Rave, K. (2012, March). Global wind report: annual market update 2011. Retrieved from http://www.gwec.net

[2] NASA. (2008). Permanent magnetic bearing for spacecraft applications. Cleveland, OH: Morales, W., Fusaro, R., & Kascak, A.

[3] Adams, M. (2001). *Rotating machinery vibration*. New York: Marcel Dekker Incorporated.

[4] Rao, S. (2004). *Mechanical vibrations*. Upper Saddle River, NJ: Pearson Education, Incorporated.

[5] Genta,G. (2005). *Dynamics of rotating systems*. New York, NY: Springer Science and Business Media Incorporated.

[6] Ham, C., Burton, M., Lin, K., & Joo, Y. (2011). Proceedings from the 15th World Multi-Conference on Systemics, Cybernetics, and Informatics: *Development of a passive magnetic bearing system for a flywheel energy storage.*

[7] Gibson, T. (2000). Magnetic bearings: an update. Retrieved from http://motionsystemdesign.com

[8] Foster-Miller Technologies. (2004). *Rotordynamics of a passive magnetic bearing system*. Albany, NY: Chen, H., Walter, T., Wheeler, T., & Lee, N.

[9] Shen, J., Tseng, K., Vilathgamuwa, D., & Chan, W. (2000). A novel compact PMSM with magnetic bearing for artificial heart application. *IEEE Transactions on Industrial Applications*, 36(4), 1061-1068.

[10] Hawkings, L. (2012). Magnetic bearings. Retrieved from http://www.calnetix.com

[11] Schweitzer, G., & Maslen, E. (Eds). (2009). *Magnetic bearings.* New York, NY: Springer Publishing.

[12] ElMadany, M., & Abduljabbar, Z. (2004). Proceedings from the Mansoura 4th International Conference: *On the dynamic analysis of rotor-bearing systems using finite elements.*

[13] Xiang, J., Chen, D., Chen, X. & He, Z. (2009). A novel wavelet-based finite element method in the analysis of rotor bearing systems. *Finite Elements in Analysis and Design, 45*, 908-916.

[14] IRD Mechanalysis, Inc. (1994). *Introduction to vibration technology.* Columbus, OH: Shreve, D.

[15] Spectraquest, Incorporated. (n.d.). *The truth behind misalignment vibration spectra of rotating machinery.* Richmond, VA: Ganeriwala, S., Patel, S., & Hartung, A.

[16] U.S. Department of Energy. (1996). Vibration testing (Contract No. DE-AC36-84CH0093). Retrieved from http://www.nrel.gov

[17] Liu, R., Liu, M., Sun, X., & Wei, Y. (2008). Proceedings from the 2008 International Conference on Embedded Software and Systems: *Signal processing and accelerometer based design for portable small displacement measurement device.* Washington, DC: IEEE.

[18] IRD Mechanalysis, Incorporated. (1995). *Signal processing for effective vibration analysis.* Columbus, OH: Shreve, D.

[19] Olsson, F. (2006). *Rotordynamic model of a fibre refinery in BEAST*. (Thesis).

Retrieved from Lulea University of Technology Publication Database.

[20] Nam, Y., & Yoon, T. (2008). Proceedings from 10th International Conference on

Control, Automation, Robotics, and Vision: *Estimation of a nacelle dynamic*

motion of a wind turbine. Hanoi, Vietnam: IEEE.

[21] Hansen, M. (2010). Wind turbine dynamics and aeroelasticity [Course Notes].

Retrieved by email.

[22] Kessentini, S., Choura, S., Najar, F., & Francher, M. (2010). Modeling and

dynamics of a horizontal wind turbine. *Journal of Vibration and Control, 16(13)*,

2001-2021.

[23] Liu, C., Jiang, D., & Chen, J. (2010). Proceedings form the 2010 World Non-grid-

connected Wind Power and Energy Conference: *Vibration characteristics of a*

wind turbine rotor using modal and harmonic analysis of FEM.

[24] Fadaeinedjad, R., Moallem, M., & Moschopoulos, G. (2008). Simulation of a wind

turbine with doubly fed induction by FAST and Simulink. *IEEE Transactions on*

Energy Conversion, 23(2), 690-700.

[25] Kusiak, A., & Zhang, Z. (2010). Analysis of wind turbine vibrations based on

SCADA data. *Journal of Solar Energy Engineering, 132*, 1-12.

[26] Vorwaller, M., Lin, K., Gou, J., Ham, C., & Joo, Y. (2012). Testbed for a wind

turbine with magnetic bearing. *Advanced Materials Research, 512,* 657-660.